

Cite this: *J. Mater. Chem. A*, 2023, 11, 22656

## Recent advances in synthesis of water-stable metal halide perovskites and photocatalytic applications†

He Zhao,<sup>a</sup> Krisztian Kordas<sup>\*b</sup> and Satu Ojala<sup>ID \*a</sup>

Solar-driven photocatalytic reactions have attracted wide interest as a viable method to generate green energy and alleviate environmental challenges posed by fossil fuels. Although, various classes of photocatalysts have been explored during the past decades, the pursuit towards even more efficient ones is still ongoing. Metal halide perovskites (MHPs) have been recently proposed as novel photocatalysts owing to their wide light absorption range and excellent optoelectronic properties. However, the instability of MHPs in water is the main obstacle that impedes their applications in practice and prompts stabilization strategies to be developed. This review focuses on the recent approaches for stabilizing MHPs in water, including surface engineering, common-ion effect, and intrinsic water stability. The photocatalytic applications of water-stable MHPs are summarized and an outlook with perspectives over the current challenges are provided.

Received 20th August 2023  
Accepted 7th October 2023

DOI: 10.1039/d3ta04994a

rsc.li/materials-a

## 1 Introduction

During recent years, the exploration of greener energy sources has become of utmost importance to alleviate the inordinate reliance on non-renewable fossil fuel reserves and the

consequent serious energy shortage and environmental pollution.<sup>1</sup> Specifically, solar radiation, as an abundant, virtually endless, and green source of energy, has been seen as a promising option for the replacement of fossil fuels.<sup>2</sup> In this context, the question of how to convert solar energy into fuels and value-added chemicals in an efficient and economic manner is a pivotal issue. So far, diverse solar-to-chemical energy conversion systems, including conventional heterogeneous photocatalysis, photoelectrochemical and combined photovoltaic-electrocatalytic systems have been proven to meet the requirements and developed for practical use.<sup>3</sup> Compared with other reported systems, photocatalytic routes are probably the

<sup>a</sup>Environmental and Chemical Engineering Research Unit, Faculty of Technology, University of Oulu, PO Box 4300, FI-90014 Oulu, Finland. E-mail: satu.ojala@oulu.fi

<sup>b</sup>Microelectronics Research Unit, Faculty of Information Technology and Electrical Engineering, University of Oulu, P. O. Box 4500, FI-90014 Oulu, Finland. E-mail: krisztian.kordas@oulu.fi

† Electronic supplementary information (ESI) available. See DOI: <https://doi.org/10.1039/d3ta04994a>



He Zhao

*He Zhao is a doctoral researcher in the Faculty of Technology at the University of Oulu. He received his BSc degree in Materials Chemistry at Zhengzhou University in 2014 and his MSc degree in Materials Physics and Chemistry from Xinjiang Technical Institute of Physics & Chemistry, University of Chinese Academy of Sciences in 2017. His current research interests include lead-free halide perovskites, semiconductor photocatalysis, 2D materials and photocatalytic hydrogen production.*



Krisztian Kordas

*Krisztian Kordas, MSc Physics and Chemistry (1998, Univ. Szeged), Dr Tech. in Microelectronics, Docent of Nanotechnology, Professor of micro- and nanoelectronic materials and components for ICT applications (2002, 2005, 2016, Univ. Oulu). He has led or participated in more than 20 national and international research projects, published 190+ papers, co-authored 6 book chapters, and supervised 11 doctoral students to graduation. His team's research is focused on synthesis, characterization, and implementation of nanostructured materials for electronics, sensors as well as for energy and environmental applications.*





## 2 Stabilization methods

Conventional lead-based MHPs are prone to decompose when exposed to moisture. It is reported that the perovskite solar cells lose more than 80% of their initial efficiency after one-day storage in ambient air, and only 5% is retained after 6 days.<sup>48</sup> Encapsulation of the MHP films using materials having diffusion barrier properties have been proposed to protect the MHP solar cells from moisture hence maintaining more than 90% of their initial performance for almost 2 months.<sup>49</sup> This is still far from the commercial long-term stability expected (25 years is typical for silicon solar cells),<sup>50</sup> thus the challenge in the MHP development remains to be solved.

To improve the water stability of MHPs, the role of water in the degradation of MHPs needs to be elucidated. The published results indicate that the MHPs adsorb water molecules quickly with a time scale of seconds<sup>51</sup> and a single water molecule can accelerate the degradation of perovskite *via* acid-base reaction.<sup>52</sup> What is even more troublesome, is that the water intake is not limited only to surface adsorption, but the water molecules also diffuse and penetrate the bulk and even infiltrate the MAPbI<sub>3</sub> unit cells (Fig. 2). However, some studies claim that MHPs have a minor tolerance to water. For example, MAPbI<sub>3</sub> was reported to remain intact when exposed to below  $2 \times 10^{10}$  Langmuir of H<sub>2</sub>O (one Langmuir equals to an exposure of about  $1.33 \times 10^{-4}$  Pa for one second).<sup>53</sup> Only ~1% volume expansion of the crystal structure is observed although water incorporated in the perovskite.<sup>54</sup> These results are consistent with previous reports of a reversible process between the hydration and dehydration stages of MAPbI<sub>3</sub>.<sup>55,56</sup> To figure out the detailed degradation mechanism under moist conditions, the dependence of spatially resolved external quantum efficiency (EQE) under various humidity exposure conditions has been investigated by using laser beam induced current mapping, and a four-stage degradation process has been proposed.<sup>57</sup> When a tiny amount of water (1.6% H<sub>2</sub>O in N<sub>2</sub>) is introduced and kept for a short time (6 min), EQE increases marginally and reaches a maximum, which is caused by the solvation of CH<sub>3</sub>NH<sub>3</sub><sup>+</sup> (MA<sup>+</sup>)

and I<sup>-</sup> ions,<sup>58</sup> that heals some defects, reduces the trap density, and thus improves the uniformity of perovskite films (Stage 1). As the time increases, a slow drop in EQE is observed due to the change of the electronic structure and carrier mobility of hole-transporting materials (Stage 2). In the next stage (Stage 3), a sharp decrease of EQE indicates the breakdown of 3D structure, while monohydrated 1-dimensional (1D) chains of CH<sub>3</sub>NH<sub>3</sub>PbI<sub>3</sub>·H<sub>2</sub>O or 0-dimensional (0D) dots of dihydrates (CH<sub>3</sub>NH<sub>3</sub>)<sub>4</sub>PbI<sub>6</sub>·2H<sub>2</sub>O are formed (Stage 3). Finally, the degradation of MHPs results in the formation of CH<sub>3</sub>NH<sub>3</sub>I (MAI), PbI<sub>2</sub> and water (Stage 4). In general, the decomposition starts at the surface, especially at the MAI-terminations.<sup>54</sup> The loss of MA<sup>+</sup> results in an open inorganic framework to form vacancies inside the crystal lattice that finally leads to a rapid deterioration or decomposition of the perovskite structure.<sup>59</sup> The dissolution of I<sup>-</sup> ions in water is easier than that of MA<sup>+</sup> ions since the hydrophobicity of -CH<sub>3</sub> group in MA<sup>+</sup> requires higher dissolution energy.<sup>60</sup> These studies indicate that water molecules penetrate easily into the bulk of MHPs and the removal of ions (especially the I<sup>-</sup> ions due to the lower energy barrier) is the main cause of the degradation. Based on the observations above, thus, the main strategies to obtain water stable MHPs are: (i) preventing the structure from the contact of water, (ii) compensating for the depletion of ions from the surrounding, and (iii) reducing the solubility of organic cations. In these efforts, three different strategies have been proposed, including surface engineering, utilization of the common-ion effect, and enhancement of the intrinsic stability of perovskites.

### 2.1 Surface engineering

Surface engineering has been explored to generate protecting layers on the MHPs, thus avoiding the direct contact of water with MHPs. In this section, six surface passivation methods are discussed: (1) organic ligands, (2) organic polymers, (3) inorganic materials, (4) metal-organic frameworks (MOFs), (5) phase engineering, and (6) water-assisted engineering.

**2.1.1 Organic ligands.** The application of organic ligands is a well-established strategy to manipulate the shape and size of

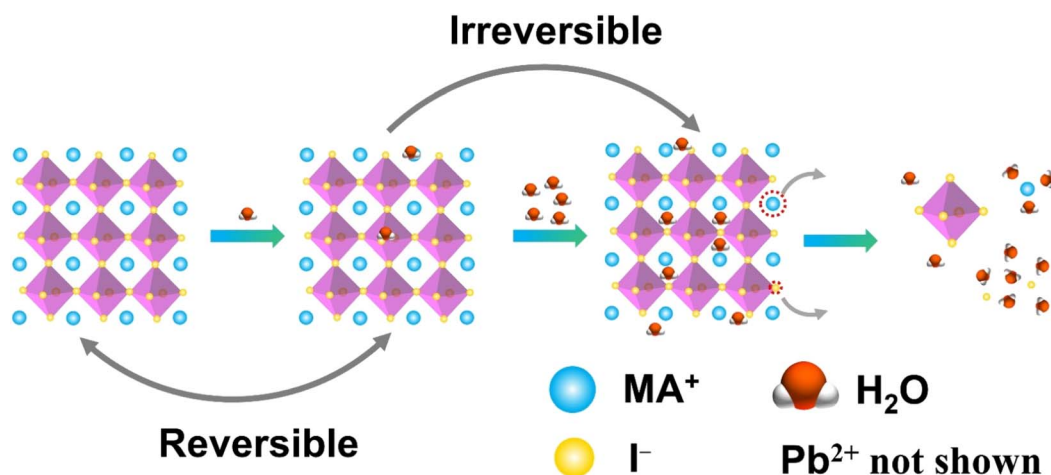


Fig. 2 Schematic illustration of MAPbI<sub>3</sub> decomposition in water.



MHP nanocrystals (NCs),<sup>61</sup> and also to stabilize MHPs.<sup>62</sup> Normally, frequently used ligands in synthesis of MHP NCs are oleic acid (OA) and oleylamine (OAm), which improve the dispersion of MHP NCs in nonpolar solvents, such as toluene and hexane. However, the dynamic adsorption-desorption process between the ligands and MHP NCs render the easy detachment<sup>63</sup> and removal of ligands in proton-donating solvents, causing the degradation of MHP NCs,<sup>64</sup> and consequent deterioration of their luminescent properties (including the electron density of states of emission bands, and the photoluminescence quantum yield).

The introduction of hydrophobic ligands on the surface of MHPs is one of the most efficient and convenient approaches to stabilize MHPs. A post-surface functionalization with hydrophobic cations *via* simple ligand exchange process can substitute surface methylammonium (MA<sup>+</sup>) ions and enhance the stability of MHPs. Many studies have indicated that the presence of hydrophobic quaternary ammonium cations, such as tetra-methyl ammonium, (CH<sub>3</sub>)<sub>4</sub>N<sup>+</sup>;<sup>65–67</sup> tetra-ethyl ammonium, (C<sub>2</sub>H<sub>5</sub>)<sub>4</sub>N<sup>+</sup>;<sup>68</sup> tetra-butyl ammonium, (C<sub>4</sub>H<sub>9</sub>)<sub>4</sub>N<sup>+</sup>;<sup>69,70</sup> and tetra-hexyl ammonium, (C<sub>6</sub>H<sub>13</sub>)<sub>4</sub>N<sup>+</sup>;<sup>71</sup> have a vital influence on the moisture-stability of MHPs. These quaternary ammonium cations adsorb chemically on the surface of MHPs, and inhibit the water intake of the lattice thus keeping the perovskite films stable under 90 ± 5% relative humidity (RH) for more than 30 days without a photovoltaic loss. This happens because the

bulky organic cations shift the surface Pb<sub>5c</sub>-I<sub>1c</sub> (I<sub>1c</sub> represents the surface I atom coordinated with one Pb atom) bonds owing to the steric effects and impede the water adsorption on the five-coordinated surface Pb atoms (Pb<sub>5c</sub>).<sup>71</sup> In addition, these molecules can also suppress the iodide migration,<sup>72</sup> evidenced by the shortened Pb-I bond (from 3.17 Å to 3.07 Å, Fig. 3a). Besides these factors, the formation of water-stable quaternary ammonium lead iodide shell may also contribute to the enhanced stability.<sup>66,73,74</sup> For example, with (C<sub>4</sub>H<sub>9</sub>)<sub>4</sub>NI post-treatment over CsPbI<sub>3</sub>, the (C<sub>4</sub>H<sub>9</sub>)<sub>4</sub>N<sup>+</sup> cations can intercalate the inorganic framework of MHP and exchange Cs<sup>+</sup> ions, forming a one-dimensional (C<sub>4</sub>H<sub>9</sub>)<sub>4</sub>NPbI<sub>3</sub> layer<sup>75</sup> exhibiting intrinsic water stability (Fig. 3b).<sup>76</sup>

Sufficient interactions between MHPs and ligands should also be considered because the instability MHP NCs partly originates from the easy detachment of ligands as described above.<sup>77</sup> Clearly, introducing reactive groups in the capping ligands and forming a covalent or ionic bonding between ligands and MHPs are deemed to improve the water stability of MHPs. For example, polyhedral oligomeric silsesquioxane (POSS) having a mercaptopropyl anchor group attaches to the surface of MHP NCs and forms a cage-like structure. Such POSS-protected CsPbX<sub>3</sub> (X = Br and/or I) NCs were shown to maintain the original green light emission and stability in water for 10 weeks.<sup>78</sup> Unlike the physical encapsulation strategy with hydrocarbons,<sup>79,80</sup> the impressive enhancement of water

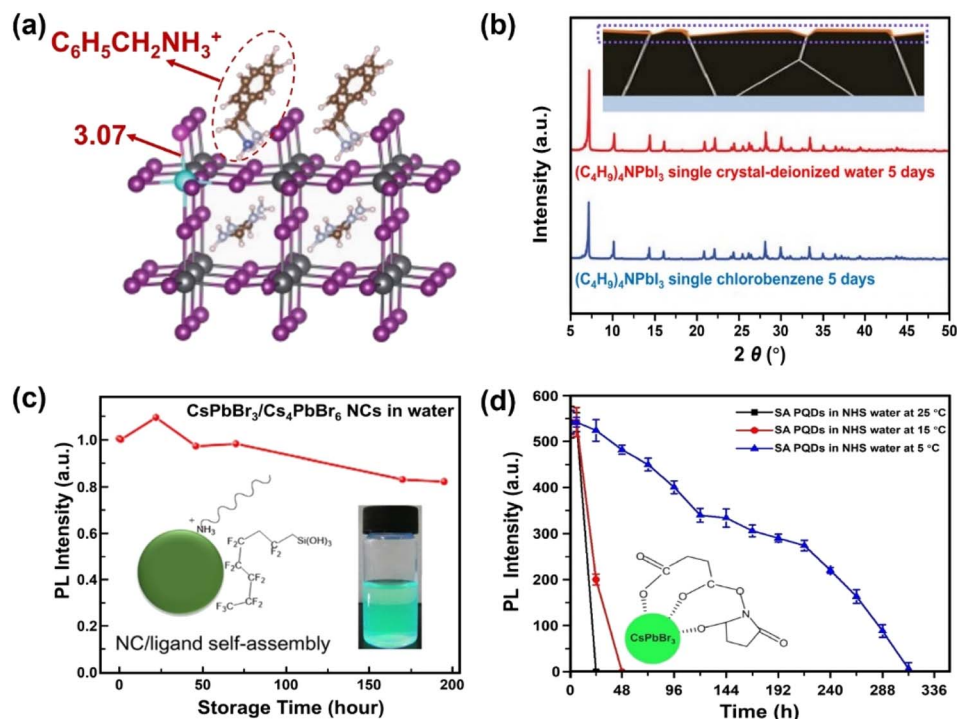


Fig. 3 Ligand engineering for water-stable MHPs. (a) Length of Pb-I bond over FA<sub>0.83</sub>Cs<sub>0.17</sub>PbI<sub>3</sub> after adding phenylmethylammonium ions. Adapted from ref. 72. (b) Formation of (C<sub>4</sub>H<sub>9</sub>)<sub>4</sub>NPbI<sub>3</sub> layers over MHP from a (C<sub>4</sub>H<sub>9</sub>)<sub>4</sub>NI post-treatment and XRD patterns of (C<sub>4</sub>H<sub>9</sub>)<sub>4</sub>NPbI<sub>3</sub> single crystals after 5 days immersion in water and toluene. Adapted from ref. 76. Copyright 2021 John Wiley and Sons. (c) Variations of PL intensity over fluorocarbon-coating CsPbBr<sub>3</sub>/Cs<sub>4</sub>PbBr<sub>6</sub> NCs in water. Adapted from ref. 86. Copyright 2018 American Chemical Society. (d) PL intensity evolution of succinic acid-capping CsPbBr<sub>3</sub> QDs in *N*-hydroxy succinimide water and the formation of tridentate ligands over QDs. Adapted from ref. 93. Copyright 2021 Elsevier.













Table 2 Water-stable MHPs obtained from polymer coatings<sup>a</sup>

Water-stable MHPs		Stability					
Materials	Methods	Medium	Characterizations	Retained PL intensity	PLQY before (after)	Observed durability	Ref.
NOA61/CH <sub>3</sub> NH <sub>3</sub> PbBr <sub>3</sub> /glass	Photocuring	Water (washing)	PL	~100%	—	Four cycles	7
CsPbBr <sub>3</sub> /PMSR (1.13 wt%)	Photocuring	Water (immersion)	PL	91%	43% (—)	24 h	122
MAPbBr <sub>3</sub> /PMSR (1.13 wt%)	Physical blending	Water (immersion)	PL	93%	53% (—)	576 h	124
MAPbBr <sub>3</sub> /PMSR (1.13 wt%)	Physical blending	Water (immersion, 70 °C)	PL	91%	53% (—)	50 min	124
MAPbBr <sub>3</sub> /PMSR (1.13 wt%)	Physical blending	Water (immersion, 100 °C)	PL	77%	53% (—)	20 min	124
MAPbBr <sub>3</sub> /SSDC (1.13 wt%)	Physical blending	Water	PL	77%	62% (—)	36 h	124
MAPbBr <sub>3</sub> /SSDC (1.13 wt%)	Physical blending	Water (immersion, 70 °C)	PL	52%	62% (—)	10 min	124
MAPbBr <sub>3</sub> /SSDC (1.13 wt%)	Physical blending	Water (immersion, 100 °C)	PL	44%	62% (—)	10 min	124
CsPbBr <sub>3</sub> NCs-PMA ( <i>R</i> <sub>pol</sub> /area of 1500)	Physical blending	Water (immersion)	PL	—	—	>8 months	128
MAPbBr <sub>3</sub> -polystyrene	Swelling-deswelling microencapsulation	Water (immersion)	PL	—	34% (32%)	2 months	129
MAPbBr <sub>3</sub> -polycarbonate	Swelling-deswelling microencapsulation	Water (immersion)	PL	—	31% (31%)	2 months	129
MAPbBr <sub>3</sub> -acrylonitrile butadiene	Swelling-deswelling microencapsulation	Water (immersion)	PL	—	48% (45%)	2 months	129
MAPbBr <sub>3</sub> -polyvinyl chloride	Swelling-deswelling microencapsulation	Water (immersion)	PL	—	16% (15%)	2 months	129
MAPbBr <sub>3</sub> -cellulose acetate	Swelling-deswelling microencapsulation	Water (immersion)	PL	—	47% (—)	2 months	129
MAPbBr <sub>3</sub> -cellulose acetate	Swelling-deswelling microencapsulation	Water (immersion)	PL	5%	—	48 h	129
MAPbBr <sub>3</sub> -poly(methyl methacrylate)	Swelling-deswelling microencapsulation	Water (immersion)	PL	—	14% (—)	2 months	129
MAPbBr <sub>3</sub> -polystyrene	Swelling-deswelling microencapsulation	Boiling water (immersion)	PL	—	34% (29%)	30 min	129
MAPbBr <sub>3</sub> -polyvinyl chloride	Swelling-deswelling microencapsulation	Boiling water (immersion)	PL	—	31% (29%)	30 min	129
CsPbBr <sub>3</sub> QDs@polystyrene	Swelling-shrinking	Water (immersion, stirring)	PL	—	68% (64.7%)	3 days	130
CsPbBr <sub>3</sub> QDs@polystyrene	Swelling-shrinking	Water (immersion, stirring)	PL	20–30%	68% (—)	30 days	130
CsPbBr <sub>3</sub> -poly(methyl methacrylate)	One-pot thermal and UV polymerization	Water (immersion)	PL	54%	54.6% (—)	48 h (30 days)	132
CsPbBr <sub>3</sub> -poly(butyl methacrylate)	One-pot thermal and UV polymerization	Water (immersion)	PL	56%	62.2% (—)	48 h (30 days)	132
MAPbX <sub>3</sub> NCs-polystyrene-poly(2-vinylpyridine) (PS- <i>b</i> -P2VP)	<i>In situ</i> growth	Water (immersion)	PL	—	—	75 days	134
Polyimide-coated CsPbBr <sub>3</sub> NCs	<i>In situ</i> growth	Water (immersion)	PL	~80%	88.1% (—)	60 min	135
MAPbBr <sub>3</sub> (8 wt%) NCs/polyvinylidene fluoride	<i>In situ</i> growth	Water (immersion)	PL	—	94.6 ± 1% (68.1 ± 1%)	400 h	136

Table 2 (Contd.)

Water-stable MHPs		Stability					
Materials	Methods	Medium	Characterizations	Retained PL intensity	PLQY before (after)	Observed durability	Ref.
Hydrolyzed poly(methyl methacrylate)-coated $\text{CH}_3\text{NH}_3\text{PbBr}_3$	Mechanical grinding	Water (suspension)	PL	~80%	—	40 days	137
$\text{CsPbBr}_3/\text{Cs}_4\text{PbBr}_6$ NCs-Hyflon-DFTHS/OLA	Physical blending	Water (suspension)	PL	68%	73% (—)	31 days	138
$\text{CsPbBr}_3$ /octylamine-modified polyacrylic acid + OAm NCs	Ligand engineering	Water (suspension)	PL	80.13%	—	15 days	139
PVP-capped $\text{CsPbX}_3$ NCs@polystyrene microhemispheres	Self-assembly	Water (washing)	PL	—	—	3 times	140
Silicone resin/PVP- $\text{CsPbBr}_3$ nanofibrous membranes	One-step electrospon	Water (immersion)	PL	—	—	Several hours	141
PS-PEB-PS and PEG-PPG-PEG coated $\text{CsPbBr}_3$ QDs	Physical blending	Water (immersion)	PL	60%	88% (86%)	1 month	142
$\text{CsPbBr}_3$ QDs-poly(styrene-ethylene-butylene-styrene) films	Physical blending	Water (immersion)	PL	—	—	122 days	143
V18-MAPBBr <sub>3</sub> NCs	Thermal polymerization	Water (immersion)	PL	85%	—	120 min	133
V18-co-MMA-MAPBBr <sub>3</sub> NCs	Thermal polymerization	Water (immersion)	PL	—	—	90 days	133
Crosslinked PETA-G/ $\text{FA}_{0.92}\text{MA}_{0.08}\text{PbI}_3$ films	Spin-coating and thermal polymerization	Water (immersion)	Photograph evolution	—	—	420 s	144
$\text{CsPbBr}_3$ /polypyrrole	Visible light polymerization	Water (immersion)	PXRD	—	—	30 days	145
$\text{CsPbBr}_3$ /polyaniline	Visible light polymerization	Water (immersion)	PL PXRD TEM	~93%	—	4 weeks	146

<sup>a</sup> NOA61: Norland Optical Adhesives 61; Ergo: Ergo® optical adhesive 8500; PMSR: phenyl methyl silicon resin; SSDC: Silicone Sealant Dow Corning® 937; PMA: poly(isobutylene-*alt*-maleic anhydride)-*graft*-dodecyl;  $R_{\text{pol/area}}$ : the number of monomers of polymer per NP area [ $\text{nm}^{-2}$ ]; Hyflo: Hyflon AD 60; DFTHS: dodecafluoroheptyl-trihydroxysilane; V18: 4-vinylbenzyl-dimethyloctadecylammonium chloride.



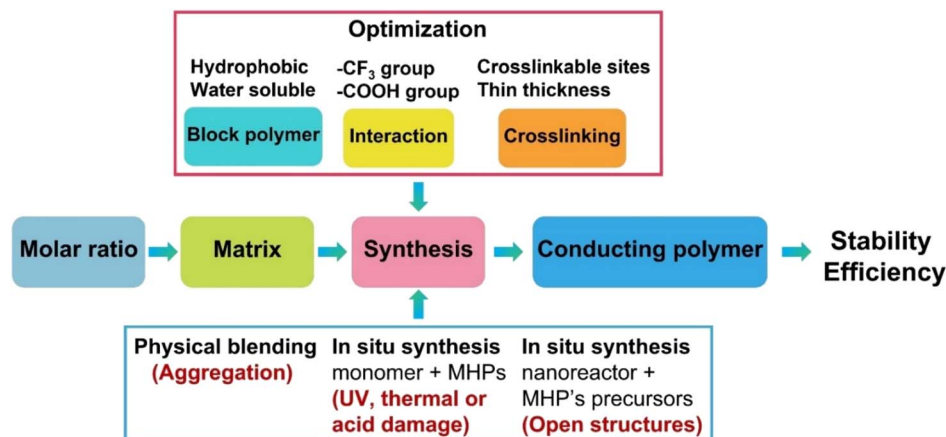


Fig. 5 Scheme of suggested strategies for the synthesis of polymer–MHPs composites.

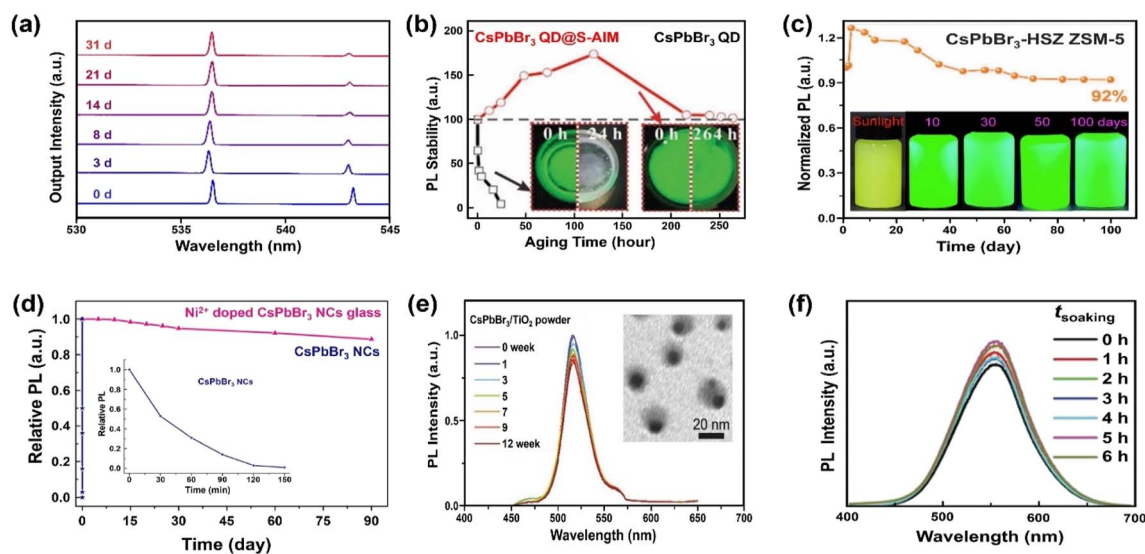


Fig. 6 Stabilizing MHPs by using inorganic materials. (a) Time-dependent normalized PL spectra of the ALD  $\text{Al}_2\text{O}_3$  coated  $\text{CsPbBr}_3$  nanoplate after being immersed in water for 1 month. Adapted from ref. 158. Copyright 2020 American Chemical Society. (b) PL intensity evolution over  $\text{CsPbBr}_3$  QDs and  $\text{CsPbBr}_3$  QDs@superhydrophobic aerogel inorganic matrix (S-AIM) completely immersed in water with time. Adapted from ref. 163. Copyright 2020 John Wiley and Sons. (c) PL stability of  $\text{CsPbBr}_3$ -HSZ ZSM-5-700 composites when exposed in water and luminescent photographs of  $\text{CsPbBr}_3$ -HSZ ZSM-5-700 composite immersed in water for various time ( $5 \text{ mg mL}^{-1}$ ). Adapted from ref. 175. Copyright 2022 Elsevier. (d) The change in relative PL of  $\text{Ni}^{2+}$  doped  $\text{CsPbBr}_3$  NCs glass and  $\text{CsPbBr}_3$  NCs in water (inset: enlarged the change of PL with  $\text{CsPbBr}_3$  NCs in water). Adapted from ref. 177. Copyright 2019 Elsevier. (e) The relative PL intensity of  $\text{CsPbBr}_3/\text{TiO}_2$  NCs after immersing in Milli-Q water (0–12 weeks), inset shows a TEM image of  $\text{CsPbBr}_3/\text{TiO}_2$  NCs after immersing in Milli-Q water for 12 weeks. Adapted from ref. 181. Copyright 2017 John Wiley and Sons. (f) Normalized PL spectra of  $\text{Cs}_2\text{Sn}_{0.89}\text{Te}_{0.11}\text{Cl}_6$  versus different soaking time. Adapted from ref. 180. Copyright 2020 John Wiley and Sons.

from rough surface,<sup>196</sup> and the hydrophobic functional groups from the AGs.<sup>163</sup>

However, the open shell after impregnation is still a threat to long-term stability. Thus, a second coating is normally needed. For this purpose, ALD grown compact  $\text{AlO}_x$ ,<sup>168</sup> polymers<sup>169,170</sup> and biomedical phospholipids<sup>171,172</sup> have been reported. The  $\text{mSiO}_2$ - $\text{CsPbBr}_3$ @ $\text{AlO}_x$  obtained with 100 ALD cycles keeps up to 95% of PL intensity after 8 h in water dispersion under stirring, and the stability extends to 90 days under static conditions.<sup>168</sup> He *et al.* embedded Mn-doped  $\text{CsPbCl}_3$  QDs into  $\text{SiO}_2/\text{Al}_2\text{O}_3$  monolith through a facile sol-gel process, followed by

a physical grinding. The obtained Mn-doped  $\text{CsPbCl}_3$  QDs- $\text{SiO}_2/\text{Al}_2\text{O}_3$  monolith sample maintained around 92% of the initial PL intensity after 7 days under accelerated aging condition ( $85^\circ\text{C}$  and 85% RH).<sup>173</sup> For polymers, this strategy can trigger the formation of micro/nano structured  $\text{SiO}_2$  surface, which is one essential feature needed for super-hydrophobicity.<sup>197,198</sup> The coating of biomedical phospholipid can also further improve the stability over  $\text{SiO}_2$  coated MHPs and broaden their applications in bioimaging and biosensing.<sup>171,172</sup>

Another issue is the aggregation during the synthesis, which may cause quenching and instability.<sup>124,199</sup> In conjunction with











Table 3 (Contd.)

Water-stable MHPs		Stability					
Materials	Methods	Medium	Characterizations	Retained PL intensity	PLQY before (after)	Observed durability	Ref.
CsPbBr <sub>3</sub> /SiO <sub>2</sub> /PEGylated phospholipid	Hydrolysis-condensation and physical blending	Water (suspension)	PL	80%	—	2 weeks	171 and 172
Mn-doped CsPbCl <sub>3</sub> QDs-SiO <sub>2</sub> /Al <sub>2</sub> O <sub>3</sub> monolith	One-pot synthesis	85 °C and 85% RH	PL	~92%	—	7 days	173
[Na <sub>4</sub> Cs <sub>8</sub> PbBr <sub>4</sub> ] <sup>18-</sup> zeolite	Ion-exchange and <i>in situ</i> growth	Water (immersion)	PL PXRD	100%	35% (—)	40 days	174
CsPbBr <sub>3</sub> QDs-HSZ ZSM-5	Grinding-calcination	Water (immersion)	PL	92%	62% (—)	100 days	175
CsPbBr <sub>1.2</sub> /I <sub>1-8</sub> NCs@P-Si-Zn glass	Melt-quenching and subsequent heat-treatment	Water (immersion)	PL	~90%	—	40 days	176
Ni <sup>2+</sup> -doped CsPbBr <sub>3</sub> NCs@B-Si-Zn glass	Melt-quenching	Water (immersion)	PL	88.2%	84.3% (—)	90 days	177
CsPbBr <sub>3</sub> QDs@TeO <sub>2</sub> -based glass	<i>In situ</i> nanocrystallization	Water (immersion)	PL	~90%	70% (—)	120 h	178
CsPbBr <sub>3</sub> QDs@TeO <sub>2</sub> -based glass	<i>In situ</i> nanocrystallization	Water (immersion)	PL	~60%	70% (—)	45 days	178
CsPbBr <sub>3</sub> @ZnO nanoparticles	Physical blending	Water (ultrasonication)	PL	—	—	30 min	179
CsPbBr <sub>3</sub> @NaYF <sub>4</sub> nanoparticles	Physical blending	Water (ultrasonication)	PL	—	—	30 min	179
Cs <sub>2</sub> Sn <sub>0.85</sub> Te <sub>0.11</sub> Cl <sub>6</sub>	Hydrothermal method	Water (immersion)	PL PXRD	100%	95.42% (—)	360 min	180
CsPbBr <sub>3</sub> /TiO <sub>2</sub>	Hydrolysis-drying	Water (immersion)	FTIR	—	—	1 week	181
CsPbBr <sub>3</sub> /TiO <sub>2</sub> core/shell NCs	Hydrolysis-calcination	Water (immersion)	XPS PL TEM PXRD	~85%	—	3 months	181

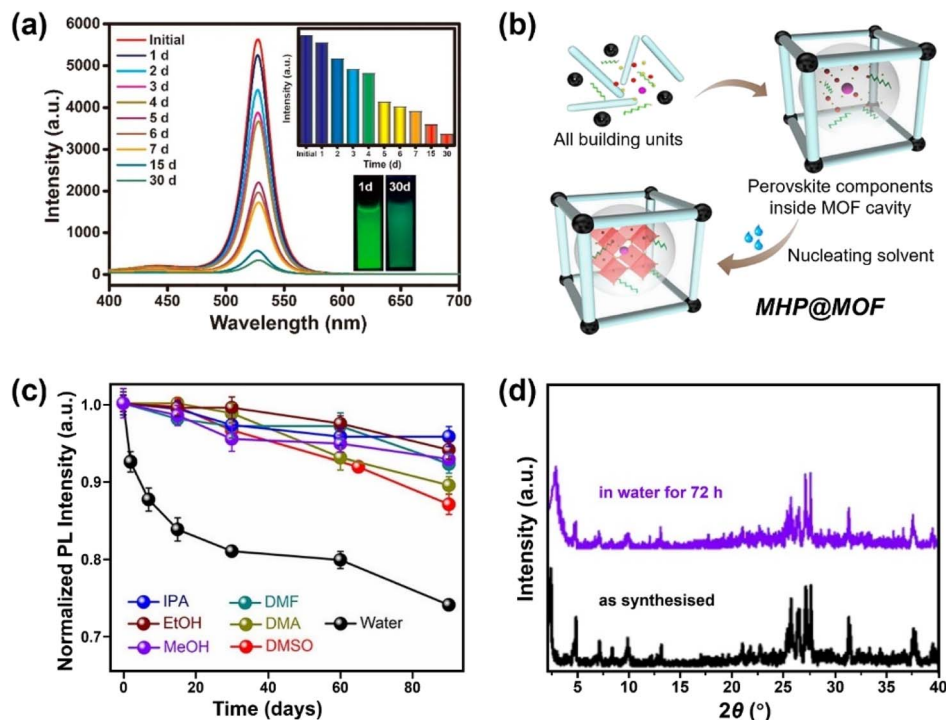


Fig. 7 MHPs encapsulated by MOF. (a) Time-dependent PL spectra of  $\text{CH}_3\text{NH}_3\text{PbBr}_3$ @MOF-5 composites in water for different days (inset: the evolution of PL intensity and the images of  $\text{CH}_3\text{NH}_3\text{PbBr}_3$ @MOF-5 composites under 365 nm light after 1 and 30 days). Reproduced with permission from ref. 213. Copyright 2018 American Chemical Society. (b) Scheme for preparing MHP@MOF composites and (c) normalized PL intensity as a function of time in different polar solvents over a period of 90 days. Adapted from ref. 215. Copyright 2019 American Chemical Society. (d) XRD patterns of  $\text{CsPbI}_3$ @PCN-222(20%) before and after immersion in water for 72 h. Adapted from ref. 218. Copyright 2022 John Wiley and Sons.

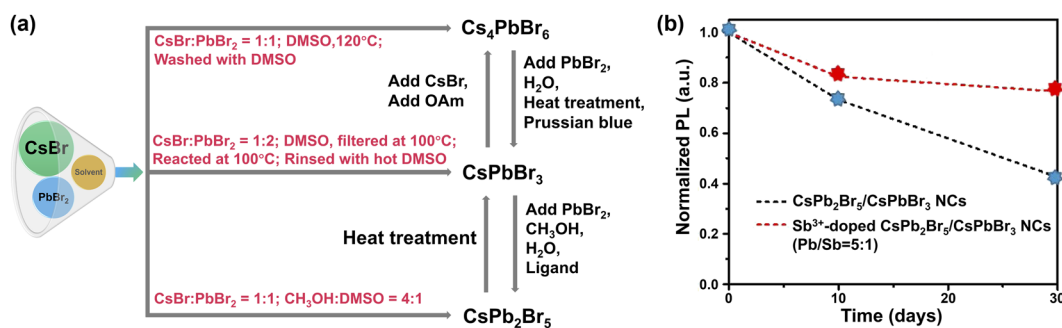


Fig. 8 Phase engineering. (a) Schematic diagram illustrating the synthesis of pure  $\text{Cs}_x\text{Pb}_y\text{Br}_z$ -based MHPs and their potential transformations. (b) PL intensity of  $\text{CsPbBr}_3/\text{CsPb}_2\text{Br}_5$  NCs and  $\text{Sb}^{3+}$ -doped dual phase  $\text{CsPbBr}_3/\text{CsPb}_2\text{Br}_5$  NCs ( $\text{Pb}/\text{Sb} = 5:1$ ) as a function of time. Adapted from ref. 237. Copyright 2021 Elsevier.

36 h storage.<sup>244</sup> This strategy was further extended to exfoliate 0D  $\text{Cs}_4\text{PbX}_6$  NCs into water-stable quasi-2D  $\text{CsPbBr}_3$  nano-sheets,<sup>245</sup> 1D  $\text{CsPbBr}_3$  nanowires, 2D  $\text{CsPbBr}_3$  nanoplatelets, and 3D  $\text{CsPbBr}_3$  nanocubes.<sup>246</sup>

The reasons for the enhanced stability are manifold. As depicted in Fig. 9a, one is the dissolution of the defective surface and thus the formation of near to ideal stoichiometry ( $\text{CsPbBr}_3$ ) having high stability.<sup>247,248</sup> Benefiting from improved crystal quality of MHP NCs and the immiscibility of hexane with water, further dissolution of  $\text{CsPbBr}_3$  NCs would not happen temporarily. Another explanation is the concurrent passivation

and the formation of halide-rich surface upon CsX-stripping.<sup>249</sup> The origin of this passivation results from the dissolution of surface layers of MHP NCs during the CsX-stripping process and subsequently the formation of non-stoichiometric MHP surface (Fig. 9b).<sup>250,251</sup> For example, with  $\text{Cs}_4\text{PbBr}_6$  NCs as starting materials, the following water treatment engenders a phase transformation into  $\text{CsPbBr}_3$ , accompanied by a passivation effect from the CsBr salt in water. The resultant  $\text{CsPbBr}_3$  NCs display ultra-stability (over 200 days with ~20% decrease in the initial PL value, Fig. 9d).<sup>250</sup> A third potential mechanism is based on the attached isomorphous hydroxyl (OH)





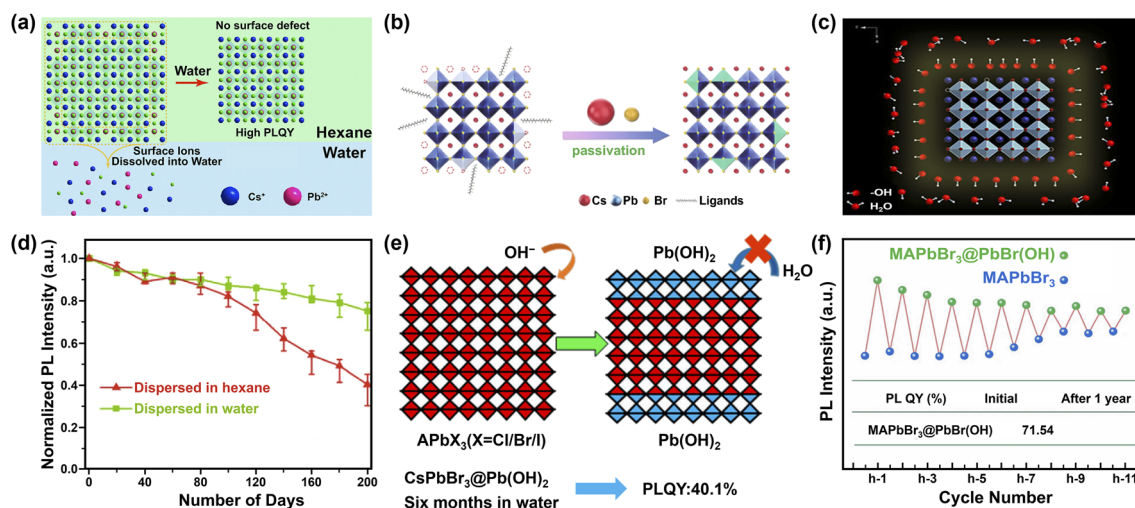


Fig. 9 Water-assisted engineering for preparing water-stable MHPs. Three possible mechanisms (a–c) for the synthesis of water-stable MHPs with water-assisted engineering strategy: (a) illustration of forming CsPbX<sub>3</sub> NCs in hexane with perfect unit cell after water-treatment. Adapted from ref. 247. Copyright 2018 American Chemical Society. (b) Schematic diagrams of CsPbBr<sub>3</sub> NCs passivated by CsBr. Reproduced with permission from ref. 250. (c) Illustration of CsPbBr<sub>3</sub> NCs stabilized by hydroxyl (OH) ligands. Reproduced from ref. 88. (d) Normalized PL intensity's evolution of CsPbBr<sub>3</sub> NCs dispersed in water and hexane respectively. Adapted from ref. 250. (e) Formation mechanism of Pb(OH)<sub>2</sub> by Lewis base vapor diffusion (LBVD) method. Adapted from ref. 259. Copyright 2018 American Chemical Society. (f) The variant PL intensity of MAPbBr<sub>3</sub>@PbBr(OH) and MAPbBr<sub>3</sub> during cycling. Adapted from ref. 261.

ligands over CsPbBr<sub>3</sub> nanocrystals that are assumed to prevent MHP NCs from further water attack (Fig. 9c).<sup>88</sup> The formation of hydroxyl might have originated from the self-ionization of water. It is reported that polar solvent (for example, isopropanol, C<sub>3</sub>H<sub>7</sub>OH) will ionize itself to produce C<sub>3</sub>H<sub>7</sub>O<sup>-</sup> and C<sub>3</sub>H<sub>7</sub>OH<sub>2</sub><sup>+</sup> and replace OA<sup>-</sup> and OAm<sup>+</sup> respectively, acting as shorter and more reactive ligands and inducing the oriented growth of MHP NCs.<sup>252</sup> Similar ionization is expected in the case of water, which triggers the formation of OH ligands on MHP NCs.<sup>253</sup> Additionally, the hydroxyl groups might provide a passivation effect by forming hydrogen bonding interaction with halide ions in MHPs.<sup>254</sup> Besides these possibilities, the formation of atomically thin quasi-2D CsPbBr<sub>3</sub> nanosheets (NSs) also favors the stability,<sup>245</sup> because the (quasi)-2D structures features improved stability<sup>255</sup> and suppressed ion migration<sup>256</sup> than their 3D counterparts.

Efforts have been devoted to decoding the underlying mechanism with density-functional theory (DFT) calculations. Recent studies indicate that Cs-rich precursor favors the formation of CsBr-terminated surface, whereas low Cs concentration results in PbBr<sub>2</sub> terminations. Compared with PbBr<sub>2</sub>-terminated surface, the former case is more stable even after the adsorption of water molecules according to the DFT results.<sup>257</sup> Yoo *et al.* proposed that a ligand transition from anionic ligands to cationic ligands in metal halide medium also contributes the improved water stability.<sup>258</sup>

*In situ* grown Pb(OH)<sub>2</sub> via a Lewis base vapor diffusion (LBVD) method has been proposed as another strategy to stabilize the MHPs (Fig. 9e).<sup>259</sup> When excess methylamine is diffused into the solution of MHPs, a basic solution (pH > 12) is formed. Then highly nucleophilic OH<sup>-</sup> ions react with the peripheral layer of [PbX<sub>6</sub>]<sup>4-</sup> on MHPs, forming a dense

Pb(OH)<sub>2</sub> layer. Notably, the as-obtained Pb(OH)<sub>2</sub>-coated perovskites maintained structural stability in water for more than 6 months and retained the fluorescence property in water even after grinding or sonication. The Pb(OH)<sub>2</sub>-coated MAPbX<sub>3</sub> perovskites can be also obtained *via* organic cation exchange between formamidinium (FA<sup>+</sup>) and MA<sup>+</sup> in water, which can further extend the stability up to one year.<sup>260</sup> Instead of the time-consuming LBVD method, to form surface hydroxides may be obtained by simply adjusting the pH of metal halide precursor solution with ammonium hydroxide.<sup>261,262</sup> Such MAPbBr<sub>3</sub>@PbBr(OH) retained 89.9% of the initial PL value (*i.e.*, 64.28%) after being immersed in water for 1 year (Fig. 9f). The PbBr(OH) layer can be also extended to all-inorganic MHPs. For example, by modulating the water content, water-stable CsPbBr<sub>3</sub>/CsPb<sub>2</sub>Br<sub>5</sub>@PbBr(OH) and CsPbBr<sub>3</sub>@PbBr(OH) nano/micro-spheres have been obtained respectively, in which CsPbBr<sub>3</sub>/CsPb<sub>2</sub>Br<sub>5</sub>@PbBr(OH) showed excellent water stability and maintained 91% of initial PL intensity after 18 months of storage in water.<sup>263</sup> Dong *et al.* also found that rod-like CsPb<sub>2</sub>Br<sub>5</sub>-embedded Pb(OH)Br obtained 92.2% of initial PL intensity after soaking in water for 165 days, indicating a good stability.<sup>264</sup> PbBrF matrix also shows good protecting ability in CsPbBr<sub>3</sub>/PbBrF composites having no decrease of PLQY after 30 days in water.<sup>265</sup> DFT calculations indicated that the improved stability originates from the increased decomposition enthalpy after introducing insoluble PbBr(OH) compared with that of bare MAPbBr<sub>3</sub> (ref. 261 and 263) or the positive energy cost for water entering the lattice of PbBr(OH).<sup>266</sup>

Even though water-assisted engineering strategy can dramatically improve MHPs stability in water, it should be mentioned that no photocatalytic applications over this class of water-stable MHPs have been reported yet.



## 2.2 Common-ion effect

It is well-known that a salt can be precipitated by adding other soluble salts having common ions to the solution. Inspired by this, Nam's group have proposed the idea of common-ion effect to prepare water-stable MHPs in aqueous solution.<sup>28</sup> Although the MHPs are stabilized, it is a difficult-to-implement strategy in the practice due to the highly corrosive nature of the solution ( $\text{pH} < -0.5$  and  $[\text{I}^-] > 2.5 \text{ mol L}^{-1}$ ). Clearly, a more practical medium is needed. Later, Geng *et al.* found that  $\text{CH}_3\text{NH}_3\text{PbX}_3$  ( $\text{X} = \text{Br}$  or  $\text{Cl}/\text{Br}$ ) nanocrystals could be synthesized in aqueous solution when the pH value was in the range of 0–5.<sup>267</sup> In this aqueous solution, the  $[\text{PbX}_6]^{4-}$  ions would adsorb on NCs, facilitating the formation of halide-rich surface of NCs, thus preventing the dissolution of MHP NCs in water. However, they would decompose in neutral solution.

To realize the water stability of MHPs, our group explored to employ the bismuth halide perovskites as photocatalysts owing to their better stability in solar cells and photocatalysis.<sup>268–270</sup> We found that the tri(dimethylammonium) hexaiodobismuthate ( $\text{DA}_3\text{BiI}_6$ ) could be stabilized in aqueous solution using dimethylammonium iodide (DAI) without addition of acids.<sup>271</sup> We noted that a stepwise transformation of  $\text{BiI}_3 \rightarrow [\text{BiI}_4]^- \rightarrow [\text{BiI}_6]^{3-}$  as the increase of DAI concentration and only  $[\text{BiI}_6]^{3-}$  ions existed when the concentration of DAI was higher than 0.15 M (Fig. 10a and b). The structural integrity of  $\text{DA}_3\text{BiI}_6$  could be preserved for more than two weeks (Fig. 10c and d). Similarly,

a series of 2D MHPs, including  $\text{C}_6\text{H}_5\text{CH}_2\text{NH}_3\text{PbI}_4$ ,  $\text{C}_6\text{H}_5(\text{CH}_2)_2\text{NH}_3\text{PbI}_4$  and  $\text{C}_6\text{H}_5(\text{CH}_2)_3\text{NH}_3\text{Pb}_2\text{I}_7$  have been stabilized in iodide salt aqueous solutions.<sup>272</sup>

## 2.3 Intrinsic water stability

Besides the strategies developed based on surface engineering and common-ion effect discussed above, exploring intrinsically water-stable MHPs are potentially advantageous because they can bypass the obstacles of water instability in aqueous media.

A few 3D MHPs have exhibited an intrinsic stability in water. As far as we know, the first reported intrinsically water-stable MHPs were hydroxyl ammonium lead iodo chloride ( $\text{OHNH}_3\text{-PbI}_2\text{Cl}$ ) and hydroxyl ammonium lead chloride ( $\text{OHNH}_3\text{-PbCl}_3$ ).<sup>273</sup> After stirring in deionized water for 1 h, no leaching of  $\text{Pb}^{2+}$  was detected. In addition, no color change of the solids was observed after a 45 days immersion in water, suggesting outstanding water-stability. It is speculated that strong hydrogen bonding interactions among MHPs contribute to the water stability. However, it is worth noting that their crystal structures are still under debate.<sup>274,275</sup> Also,  $\text{C}_6\text{H}_4\text{NH}_2\text{CuBr}_2\text{I}$  with  $\text{ABX}_3$  structure has exhibited no structure change after water immersion for 4 h.<sup>276,277</sup> Currently, another widely studied water-stable MHPs are dimethylammonium tin halide perovskites,<sup>278,279</sup> which feature no decomposition after 20 h in deionized water (see Fig. 11a). Based on DFT calculations (Fig. 11b), the intrinsic water-stability originates from higher

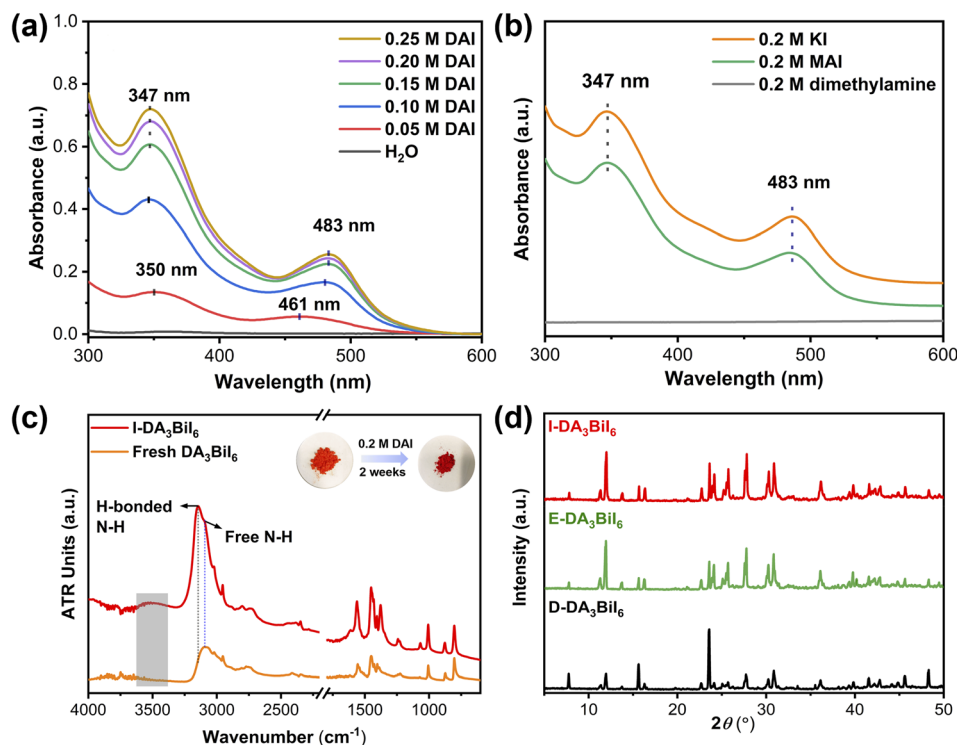


Fig. 10 Common-ion effect. (a) UV-vis absorption spectra of DAI aqueous solutions after immersing  $\text{DA}_3\text{BiI}_6$  for 1 day. (b) UV-vis absorption spectra of 0.2 M aqueous dimethylamine, KI, and MAI solutions after immersing  $\text{DA}_3\text{BiI}_6$  for 5 min. (c) ATR-FTIR spectra and color change of  $\text{DA}_3\text{BiI}_6$  and immersed- $\text{DA}_3\text{BiI}_6$  powder. (d) XRD patterns of  $\text{DA}_3\text{BiI}_6$  after immersion in water, ethanol and  $\text{DA}_3\text{BiI}_6$  synthesized from DAI. Reproduced from ref. 271.



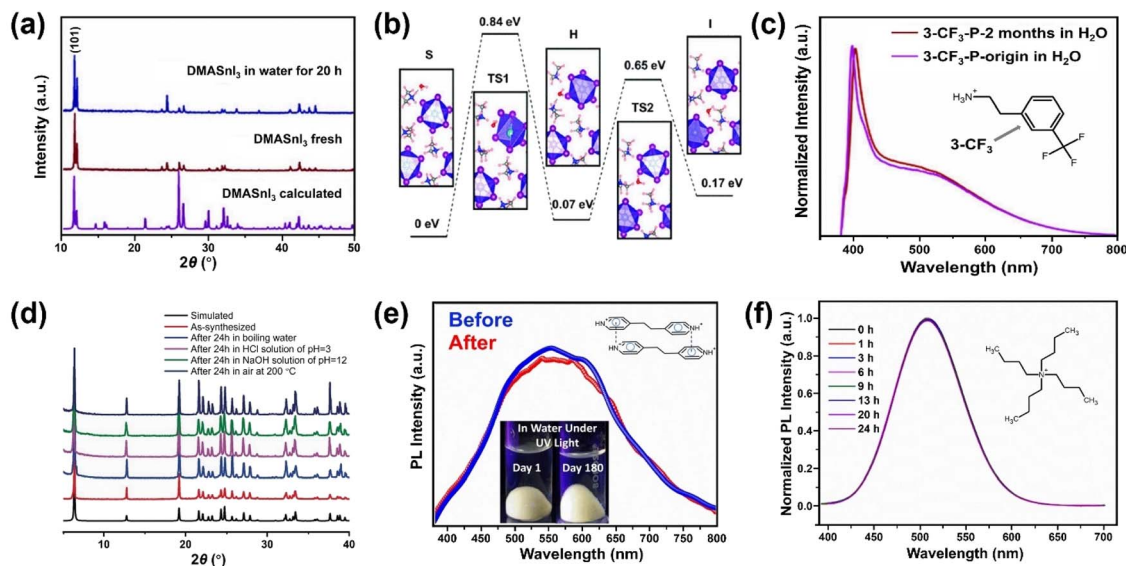


Fig. 11 Intrinsic water-stable MHPs. (a) The powder XRD (PXRD) patterns of DMASnI<sub>3</sub> before and after water treatment. Adapted from ref. 279. Copyright 2020 John Wiley and Sons. (b) Relative energy profile for water infiltration into (101) surface of DMASnI<sub>3</sub> crystal. Adapted from ref. 279. Copyright 2020 John Wiley and Sons. (c) PL spectra of 3-CF<sub>3</sub>-MHP before and after being kept in water for 2 months. Adapted from ref. 285. Copyright 2022 American Chemical Society. (d) PXRD patterns of [Pb<sub>2</sub>Cl<sub>2</sub>]<sup>2+</sup> [O<sub>2</sub>C(CH<sub>2</sub>)<sub>2</sub>CO<sub>2</sub>]<sup>-</sup> before and after chemical treatment for 24 h. Adapted from ref. 288. Copyright 2017 John Wiley and Sons. (e) PL spectra of fresh and immersed (4,4'-EDP)Pb<sub>2</sub>Br<sub>6</sub> for 180 days. Adapted from ref. 294. Copyright 2021 John Wiley and Sons. (f) Normalized PL spectra evolution of (C<sub>4</sub>H<sub>9</sub>)<sub>4</sub>NCuCl<sub>2</sub> after water immersion for different periods. Adapted from ref. 296. Copyright 2021 American Chemical Society.

water surface adsorption energy, higher water osmotic energy barrier, and smaller intralayer spacing inside DMASnI<sub>3</sub> structure compared with the Pb-based counterpart.<sup>279</sup>

In contrast to 3D MHPs, low-dimensional (2D, 1D and 0D) perovskites have shown better environmental stability.<sup>280–282</sup> A typical 2D perovskite can be regarded as interdigitating bulky organic bilayers intercalated by inorganic layers. The replacement of MA<sup>+</sup> with bulkier alkylammonium cations results in enhanced stability.<sup>255</sup> Inspired by this, several (quasi-) 2D perovskites having a bulky organic cation, *e.g.*, phenylethylammonium (C<sub>8</sub>H<sub>9</sub>NH<sub>3</sub><sup>+</sup>, PEA<sup>+</sup>),<sup>283–285</sup> 1-hexadecylammonium (CH<sub>3</sub>(CH<sub>2</sub>)<sub>15</sub>NH<sub>3</sub><sup>+</sup>, HDA<sup>+</sup>),<sup>286</sup> have been developed (Fig. 11c). Among them, PEA-based MHPs have been widely investigated and proven that increased van der Waal's interactions<sup>255</sup> and reduced water adsorption energy are the key factors for the improved stability.<sup>283</sup> Another possibility is to have a better interaction between the A site (such as cysteamine,<sup>287</sup>  $\alpha,\omega$ -alkanedicarboxylates [O<sub>2</sub>C(CH<sub>2</sub>)<sub>4</sub>CO<sub>2</sub>]<sup>-</sup>,<sup>288,289</sup> bipyridine<sup>290</sup>) and inorganic framework (Fig. 11d).<sup>288</sup> As supported by DFT calculations, the strong coordination between Pb atoms and adipate dianions increases the energy cost of surface hydrolysis and limits the penetration of water molecules.<sup>289</sup>

Meanwhile, a series of 1D and 0D MHPs with intrinsic water stability have been reported including 1D [N-methyldabconium]PbI<sub>3</sub>,<sup>291</sup> [(AD)Pb<sub>2</sub>Cl<sub>5</sub>],<sup>292</sup> (DAO)Sn<sub>2</sub>I<sub>6</sub> (DAO = 1,8-octyldiammonium),<sup>293</sup> (4,4'-TMDP)Pb<sub>2</sub>Br<sub>6</sub> (TMDP = trimethylenedipyridinium),<sup>294</sup> (4,4'-EDP)Pb<sub>2</sub>Br<sub>6</sub> (EDP = ethylenedipyridinium),<sup>294</sup> and 0D (3-ethylbenzo[d]thiazol-3-ium)<sub>4</sub>Bi<sub>2</sub>I<sub>10</sub>,<sup>295</sup> (C<sub>4</sub>H<sub>9</sub>)<sub>4</sub>NCuCl<sub>2</sub>.<sup>296</sup> The cations are summarized in Fig. 12, and the details of stability are listed in Table 4. The molecular design strategies aim to increase the ionization energy,<sup>291</sup> introduce

cation- $\pi$  interaction (Fig. 11e),<sup>294</sup> enhance steric hindrance effect (Fig. 11f),<sup>292,296</sup> or utilize hydrogen-bond-free A sites.<sup>295</sup> Among them, one report introduced the concept of long-range intermolecular cation- $\pi$  interactions among A-site cations (4,4'-TMDP or 4,4'-EDP) of hybrid perovskites and facilitate the formation of polymer-like network, imparting water stability up to 180 days (Fig. 11e). Cation- $\pi$  interaction is originated from the noncovalent interaction between the  $\pi$  face of aromatic ring and cation (such as alkali cations, ammonium ions),<sup>297</sup> which is stronger than the cation-water interactions during the decomposition of MHPs.<sup>298</sup> Undoubtedly, the development of intrinsic stability of MHPs in water may provide new directions and opportunities to advance the photocatalytic applications.

Besides the selection of A cations, substitution of the B sites with smaller divalent metals could reduce the lattice parameter and increase the cohesive energy, which has been reported to improve the MHP stability.<sup>299–301</sup> Substitution of Pb<sup>2+</sup> with smaller divalent metals would also favor the formation of vacancy-ordered A<sub>2</sub>BX<sub>6</sub> double perovskites with improved stability. Hamdan *et al.* synthesized a vacancy ordered halide perovskite Cs<sub>2</sub>PtI<sub>6</sub> exhibiting extraordinary stability up to 1 year under ambient condition and showing stability under high temperature (350 °C), extremely acidic (pH 1) and basic (pH 13) solutions.<sup>302</sup> DFT calculations suggest that the improved stability is due to the strong covalent interaction of the B-X bonds in the isolated [BX<sub>6</sub>]<sup>2-</sup> clusters.<sup>303</sup>

Halogen anion substitution is another approach. A partial replacement of iodide with bromide was found to enhance stability and water tolerance in mixed iodide-bromide MHP compositions.<sup>304</sup> This is related to the suppression of oxygen incorporation and the presence of stronger hydrogen bonds



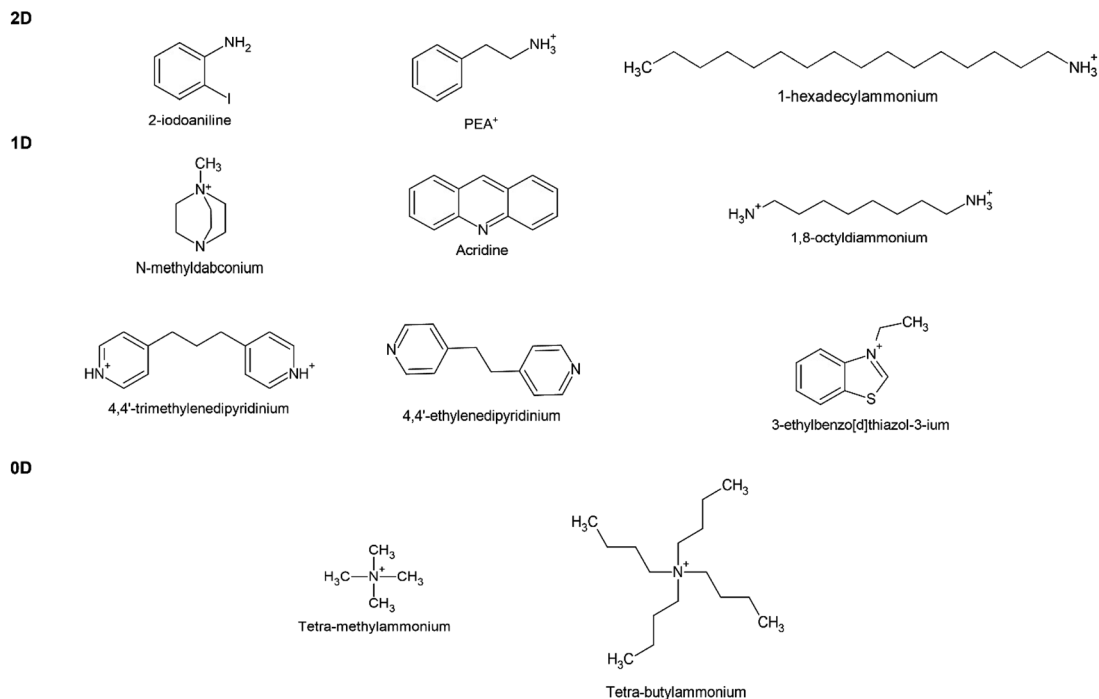


Fig. 12 Chemical structures of organic cations used for fabricating water-stable MHPs.

between the MA<sup>+</sup> cation and Br<sup>-</sup> ions as the bromide content increases<sup>305</sup> as well as the weaker interaction of water with bromide.<sup>306</sup> Apart from halogen ions, pseudohalides (cyanide, cyanate, thiocyanate, selenocyanate, azide, BF<sub>4</sub><sup>-</sup>, PF<sub>6</sub><sup>-</sup>, BH<sub>4</sub><sup>-</sup>, N<sub>3</sub><sup>-</sup> and HCOO<sup>-</sup>) have shown significant stability enhancement of MHPs.<sup>307</sup> For instance, thiocyanate (SCN)-substituted CH<sub>3</sub>-NH<sub>3</sub>Pb(SCN)<sub>2</sub>I was shown to be more stable than pristine CH<sub>3</sub>NH<sub>3</sub>PbI<sub>3</sub> (for 4 h vs. <1.5 h) under 95% humidity.<sup>309</sup>

### 3 Photocatalytic applications

In the past seven years, water-stable MHPs have attracted much attention for numerous potential applications (Table S1 and Fig. S1†) owing to their enhanced stability and improved performance. Very recently, it has been exploited as potential photocatalysts in different reactions. In this section, we will provide an overview of these photocatalytic applications and will show lots of nice and encouraging studies for pollutant degradation, H<sub>2</sub> generation, CO<sub>2</sub> reduction and organic synthesis over water-stable MHP photocatalysts.

#### 3.1 Pollutant degradation

Photocatalytic degradation is an attractive way to remove pollutants from wastewater and thus a great amount of work has been devoted to exploring effective photocatalysts. Aamir *et al.* firstly reported on water-stable OHNH<sub>3</sub>PbI<sub>2</sub>Cl and OHNH<sub>3</sub>PbCl<sub>3</sub> for photocatalytic dye degradation of Direct Yellow 27 dye under sunlight with a degree of degradation of 93.98% within 20 min and almost 100% after 55 min, respectively.<sup>273</sup> However, both catalysts are only UV-responsive. On the other hand, Ghosh and co-workers reported that the water-

stable MAPbBr<sub>3</sub>@ZIF-8 composites could degrade different pollutants (methyl orange, methyl red and nitrofurazone) under visible light (60 W LED lamp, λ<sub>max</sub> ~ 530 nm) or sunlight. The composite exhibited a higher degradation for methyl orange and could degrade methyl orange up to 90% in 100 min (degradation rate constant: 0.02723 min<sup>-1</sup>), shown in Fig. 13a.<sup>215</sup> Although the degradation rate is not high enough compared to the other materials, it can be improved by using photoactive MOFs.<sup>310</sup>

To alleviate the toxicity associated with Pb, some lead-free MHPs have been explored. Wu *et al.* prepared a C<sub>6</sub>H<sub>4</sub>NH<sub>2</sub>CuCl<sub>2</sub>I film to degrade rhodamine B (RhB) under visible light irradiation. Degradation of 18% of RhB in 60 min was achieved (degradation rate constant: 0.003 min<sup>-1</sup>). They found that the sluggish transfer rate of holes restrains photocatalytic performance of this catalyst. After coupling the photocatalyst with a hole-transporting material (CuO), the charge separation was enhanced, resulting in a degradation rate of 0.005 min<sup>-1</sup>.<sup>311</sup> As also suggested by the study, one may enhance the overall photocatalytic activity by constructing heterojunctions that rectify electron-hole transport at the interface of two semiconductors to facilitate better charge separation and to limit photocharge recombination. A good example is a nanocomposite of PEA<sub>2</sub>SnBr<sub>4</sub>/g-C<sub>3</sub>N<sub>4</sub> prepared *via* ball milling of the constituents. Compared with pristine g-C<sub>3</sub>N<sub>4</sub>, the heterojunction decreased the degradation time of methylene blue (10<sup>-5</sup> M) from 90 min to 45 min (degradation rate constant: 0.078 min<sup>-1</sup>) under solar light.<sup>284</sup> Among the so far reported photocatalysts, DMASnI<sub>3</sub> seems to show the best photocatalytic performance with a complete conversion of methyl orange (100 mg L<sup>-1</sup>) in 12–15 min (degradation constant rate: ~0.13 min<sup>-1</sup>) under visible light.<sup>279</sup>



Table 4 Summary of intrinsically water-stable MHPs<sup>a</sup>

Water-stable MHPs		Stability					
Materials	Methods	Medium	Characterizations	Retained PL intensity	PLQY before (after)	Observed durability	Ref.
(C <sub>4</sub> H <sub>9</sub> ) <sub>4</sub> NPbI <sub>3</sub> NBCAnPbI <sub>3</sub> (CH <sub>3</sub> NH <sub>2</sub> PbI <sub>3</sub> ) <sub>3</sub>	Solvent evaporation	Water (immersion)	PXRD	—	—	5 days	76
	<i>In situ</i> synthesis	Water (immersion)	UV-vis absorption spectroscopy	—	—	30 min	73
Rb <sub>0.05</sub> Cs <sub>2.95</sub> Bi <sub>2</sub> I <sub>9</sub> single crystals	Temperature lowering method	Water (immersion)	PL, PXRD, XPS and UV-vis absorption spectroscopy	~100%	17.63% (—)	24 h	308
OHNH <sub>3</sub> PbI <sub>2</sub> Cl crystals	Solution method	Water (stirring)	UV-vis absorption spectroscopy	—	—	45 days	273
	Solution method	Water (stirring)	UV-vis absorption spectroscopy	—	—	45 days	273
C <sub>6</sub> H <sub>4</sub> NH <sub>2</sub> CuBr <sub>2</sub> I thin film	Grinding and spin-coating	Water (immersion)	PXRD	—	—	4 h	276
C <sub>6</sub> H <sub>4</sub> NH <sub>2</sub> CuBr <sub>2</sub> I thin film	—	Water (immersion)	PXRD	—	—	2 h	277
(CH <sub>3</sub> ) <sub>2</sub> NH <sub>2</sub> SnI <sub>3</sub> (DMASnI <sub>3</sub> ) single crystals	Temperature lowering method	Water (immersion)	UV-vis absorption spectroscopy	—	—	16 h	278
	Temperature lowering method	Water (immersion)	PXRD	—	—	20 h	279
DMASnI <sub>x</sub> Br <sub>3-x</sub> crystals	—	Water (immersion)	PXRD, XPS, FTIR	—	—	—	—
Mn-doped (PEA) <sub>2</sub> PbBr <sub>4</sub> crystals	Lewis base-assisted precipitated method	Water (immersion)	UV-vis diffuse reflectance spectroscopy	—	>45% (—)	45 days	283
	Wet-chemistry (solvent evaporation)	Water (stirring)	High-power XRD	—	—	4 h	284
Trifluoromethyl-modified PEA <sub>2</sub> PbBr <sub>4</sub> (HDA) <sub>2</sub> PbI <sub>4</sub> (HDA <sup>+</sup> = CH <sub>3</sub> (CH <sub>2</sub> ) <sub>15</sub> NH <sub>3</sub> <sup>+</sup> ) (HCya) <sub>2</sub> PbI <sub>4</sub> (Cya = HS(CH <sub>2</sub> ) <sub>2</sub> NH <sub>2</sub> ) crystals [Pb <sub>2</sub> X <sub>2</sub> <sup>2+</sup> ] [O <sub>2</sub> C(CH <sub>2</sub> ) <sub>4</sub> CO <sub>2</sub> <sup>-</sup> ] crystals	Temperature lowering method	Water (immersion)	PXRD	~100%	18.11% (—)	74 days	285
	Modified ligand-assisted reprecipitation	Water (immersion)	ICP-OES	—	—	30 min	286
	Temperature lowering method	50% isopropanol-water (immersion)	PL	—	—	>30 s	287
	Hydrothermal method	Boiling water, HCl solution (pH 3), and NaOH solution (pH 12)	PXRD	—	—	24 h	288



Table 4 (Contd.)

Water-stable MHPs		Stability					
Materials	Methods	Medium	Characterizations	Retained PL intensity	PLQY before (after)	Observed durability	Ref.
$[\text{Pb}_2\text{X}_2^{2-}]$ $[\text{O}_2\text{C}(\text{CH}_2)_4\text{CO}_2^-]$ crystals	Hydrothermal method	HCl solution (pH 3–6), pure water (pH 7) NaOH solution (pH 8–11) and boiling water	PXRD	—	—	24 h	289
$\text{APbX}_2$ (A = bipyridine) crystals	Ligand-assisted reprecipitation	Water (immersion)	PXRD XPS SEM	—	—	24 h	290
$[\text{N-Methyl(dabconium)]PbI}_3$ crystals	Solvent evaporation	Water (immersion)	PXRD Dielectric permittivity	—	—	15 h	291
$[\text{AD}]\text{Pb}_2\text{Cl}_5$ (AD = acridine) micro-belts	Precipitation	Water (immersion)	PL PXRD SEM	~100%	7.45% (58.79%)	60 days	292
$(\text{DAO})\text{Sn}_2\text{I}_6$ (DAO = 1,8-octyldiammonium) crystals	Temperature lowering method	Water (immersion)	XPS UV-vis absorption and Raman spectra, PXRD	—	20.3% (—)	>15 h	293
4,4'-Trimethylenedipyridinium lead bromide crystals $[(4,4'\text{-TMDP})\text{Pb}_2\text{Br}_6]$	Temperature lowering method	Water (immersion)	PL UV-vis absorption, PXRD	~100%	3.7% (—)	180 days	294
4,4'-Ethylenedipyridinium lead bromide crystals $[(4,4'\text{-EDP})\text{Pb}_2\text{Br}_6]$	Temperature lowering method	Water (immersion)	PL UV-vis absorption, PXRD	~100%	4% (—)	180 days	294
(3-Ethylbenzo[d]thiazol-3-ium) $_4$ Bi $_2$ I $_{10}$ ( $\text{EtbtBi}_{10}$ ) single crystals	Solvent evaporation	Water (immersion)	PL XPS PXRD	98.6%	82% (—)	24 h	296
$(\text{C}_4\text{H}_9)_4\text{NCuCl}_2$ single crystals	Solvent evaporation	Water (immersion)	PXRD	—	—	4 h	302
$\text{Cs}_2\text{Pt}_6$ $\text{CH}_3\text{NH}_3\text{Pb}(\text{SCN})_3\text{I}$	Hydrothermal method Solvent evaporation	Water (immersion) 95% RH	UV-vis absorption spectra	—	—	4 h	309

<sup>a</sup> NBCAnPbI<sub>3</sub>: 4-[(N-3-butylne)carboxyamido]anilinium lead(II) iodide; ICP-OES: inductively coupled plasma optical emission spectrometry.

### 3.2 H<sub>2</sub> evolution reaction (HER)

MHPs have also been regarded as a promising family of materials for photocatalytic HER. However, due to the constraint of water stability, previous works in MHP photocatalysts mainly focused on hydrogen generation from concentrated halide acids as summarized before.<sup>40–47</sup> Here, the results related to MHP-based photocatalysts for H<sub>2</sub> production from water are presented. The first results of H<sub>2</sub> evolution from water with MHPs was reported by Tao's group<sup>278</sup> using DMASnI<sub>3</sub>, H<sub>2</sub> evolution from water under 300 W Xe-lamp was explored and H<sub>2</sub> evolution rate of 3.2 μmol g<sup>-1</sup> h<sup>-1</sup> was obtained. One year later, Malavasi's group observed that DMASnBr<sub>3</sub> is also highly air-resistant.<sup>312</sup> They proved that bare DMASnBr<sub>3</sub> photocatalyst exhibited a HER rate of 6 μmol g<sup>-1</sup> h<sup>-1</sup> (50 mW cm<sup>-2</sup>, 1500 W Xenon lamp with UV filter), which was further improved to 11 μmol g<sup>-1</sup> h<sup>-1</sup> after introducing triethanolamine (TEOA) as sacrificial agent and 1 wt% Pt as co-catalyst. Later, g-C<sub>3</sub>N<sub>4</sub> was introduced to further improve the HER performance by constructing heterojunctions. As shown in Fig. 13b, the DMASnBr<sub>3</sub>@g-C<sub>3</sub>N<sub>4</sub> (33 wt% DMASnBr<sub>3</sub>) exhibited stable HER activities and reached an impressive H<sub>2</sub> production of 1730 μmol g<sup>-1</sup> h<sup>-1</sup> with an apparent quantum yield (AQY) of 6.6% (50 mW cm<sup>-2</sup>, 1500 W Xenon lamp with UV filter).<sup>313</sup> The enhancement of photocatalytic activity is closely tied to the suitable bandgap and matched band alignment. Same strategy was extended to PEA<sub>2</sub>SnBr<sub>4</sub>/g-C<sub>3</sub>N<sub>4</sub> and Cs<sub>3</sub>Bi<sub>2</sub>Br<sub>9</sub>/g-C<sub>3</sub>N<sub>4</sub> systems and the maximum HER rates of 1600 μmol g<sup>-1</sup> h<sup>-1</sup> (50 mW cm<sup>-2</sup>,

1500 W Xenon lamp with UV filter) and 1050 μmol g<sup>-1</sup> h<sup>-1</sup> (50 mW cm<sup>-2</sup>, 1500 W Xenon lamp with UV filter) were achieved, respectively.<sup>284,314</sup> Apart from hydrid MHPs, inorganic MHPs have also been employed as photocatalysts for HER due to their better stability in humid air.<sup>315</sup> Yin *et al.* prepared a series of inorganic Cs<sub>2</sub>Pt<sub>x</sub>Sn<sub>1-x</sub>Cl<sub>6</sub> (0 ≤ x ≤ 1) crystals *via* a hydrothermal method. The Cs<sub>2</sub>Pt<sub>0.05</sub>Sn<sub>0.95</sub>Cl<sub>6</sub> catalyst exhibited good phase stability in water for at least 4 hours and obtained a rate of 16.11 μmol g<sup>-1</sup> h<sup>-1</sup> (300 W Xe lamp) for hydrogen evolution from water using TEOA as the sacrificial agent.<sup>209</sup> Encouragingly, Fei's group reported the first organolead iodide layered crystalline material [Pb<sub>8</sub>I<sub>8</sub>(H<sub>2</sub>O)<sub>3</sub>]<sup>8+</sup>[<sup>-</sup>O<sub>2</sub>C(CH<sub>2</sub>)<sub>4</sub>CO<sub>2</sub>]<sup>-</sup><sub>4</sub> (TJU-16) with overall photocatalytic water splitting characteristics few years ago. Combing Rh as co-catalysts, the TJU-16-Rh<sub>0.22</sub> exhibited a hydrogen evolution rate of 31 μmol g<sup>-1</sup> h<sup>-1</sup> (300 W Xenon lamp with an AM1.5 G filter) with AQY of 0.13% at 320 nm.<sup>289</sup>

### 3.3 CO<sub>2</sub> reduction

To alleviate environmental issues related to ever-increasing levels of CO<sub>2</sub> concentration in the atmosphere, photocatalytic valorization of CO<sub>2</sub> to useful compounds such as CO, methane, formic acid and alike have been placed in the focus of research for decades. Recently, Chen *et al.* combined water-stable perovskite-like organolead iodide [Pb<sub>8</sub>I<sub>8</sub>(H<sub>2</sub>O)<sub>3</sub>]<sup>8+</sup>[<sup>-</sup>O<sub>2</sub>C(CH<sub>2</sub>)<sub>4</sub>CO<sub>2</sub>]<sup>-</sup><sub>4</sub> (TJU-16) with Au co-catalyst (Au<sub>0.19</sub>/TJU-16) for photocatalytic CO<sub>2</sub> reduction in aqueous solution.<sup>316</sup> Without using any sacrificial agent, the Au<sub>0.19</sub>/TJU-16 with loading of 0.19 wt% of Au

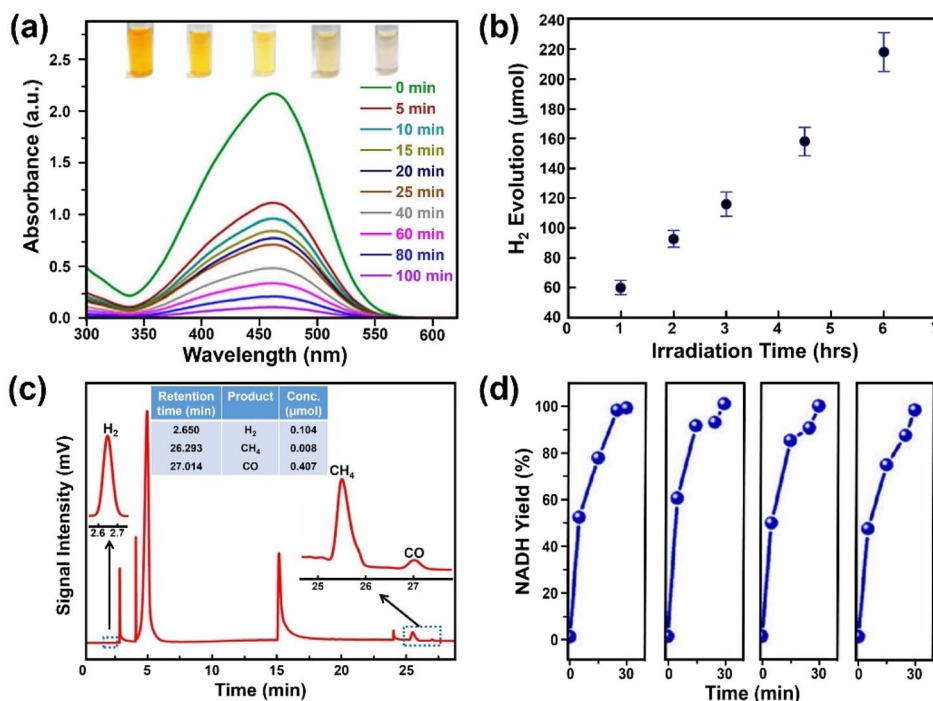


Fig. 13 Photocatalytic applications over water-stable MHPs. (a) Absorption spectra evolution of methyl orange solution degraded by MAPbBr<sub>3</sub>@ZIF-8 under visible light irradiation. Adapted from ref. 215. Copyright 2019 American Chemical Society. (b) Hydrogen evolution over 33 wt% DMASnBr<sub>3</sub>@g-C<sub>3</sub>N<sub>4</sub> composite (1 g L<sup>-1</sup>, 10% v/v triethanolamine, 3 wt% Pt) under simulated solar light. Adapted from ref. 313. Copyright 2020 John Wiley and Sons. (c) CO<sub>2</sub> reduction products over CsPbBr<sub>3</sub>@g-C<sub>3</sub>N<sub>4</sub> composite under AM1.5 G simulated sunlight. Adapted from ref. 317. Copyright 2022 Elsevier. (d) Nicotinamide adenine dinucleotide (NADH) yields over DMASnI<sub>3</sub> irradiated by blue LED lamp (wavelength of 450 nm) with four independent tests. Adapted from ref. 279. Copyright 2020 John Wiley and Sons.



nanoparticles showed the highest photocatalytic CO production rate of  $2.5 \mu\text{mol g}^{-1} \text{h}^{-1}$  and  $\text{CH}_4$  production rate of  $10.1 \mu\text{mol g}^{-1} \text{h}^{-1}$  in water under AM 1.5 G simulated irradiation, achieving a solar-to-fuel conversion efficiency of 0.034%. In addition, the consumption of electrons calculated from CO and  $\text{CH}_4$  of  $\text{Au}_{0.19}/\text{TJU-16}$  is 2.2-fold of individual TJU-16. It was concluded that the improvement in the activity originated from the spatial charge accumulation and enhanced interfacial charge transfer when applying the Au co-catalyst. In another study, photocatalyst film of  $\text{CsPbBr}_3$  nanoparticles coated with monolayered  $\text{C}_3\text{N}_4$  ( $\text{CsPbBr}_3@g\text{-C}_3\text{N}_4$ ) was found to be capable of transforming  $\text{CO}_2$  to CO,  $\text{CH}_4$  and  $\text{H}_2$  ( $0.407$ ,  $0.104$  and  $0.008 \mu\text{mol cm}_{\text{cat}}^{-2}$ , respectively) in the presence of water vapor under AM1.5 G solar without using scavengers.<sup>317</sup> Nanoparticles of the individual phases (*i.e.*,  $g\text{-C}_3\text{N}_4$  or  $\text{CsPbBr}_3$ ) alone did not produce any reduction species of  $\text{CO}_2$  (Fig. 13c). Isotopic labeling experiments confirmed the origin of products from  $\text{CO}_2$  reduction. The improved performance was ascribed to the enhanced stability of  $\text{CsPbBr}_3$  coated with the  $g\text{-C}_3\text{N}_4$  shell as well as by the promoted separation of photocarriers at the heterojunction interface.

Doping of the photocatalyst with ionic impurities offers a further strategy to improve their optical absorption, catalytic behavior as well as carrier transport properties.<sup>87,251</sup> For example, Co-doped  $\text{CsPbBr}_3/\text{Cs}_4\text{PbBr}_6$  NCs was demonstrated to be superior compared to its pristine counterpart for water-assisted  $\text{CO}_2$  photoreduction with a conversion of  $247 \mu\text{mol g}^{-1}$  under visible light irradiation (with CO and  $\text{CH}_4$  as the main products). The Co-dopant is assumed to provide not only additional active sites, but it is also believed to be responsible for altering the adsorption energies of reactants and intermediates thus influencing the reaction pathways.

### 3.4 Organic synthesis

Photocatalytic synthesis of organic compounds is another fascinating field to offer environmentally benign and cost-effective routes. Although numerous works have been done with MHPs for organic synthesis, such as C-X ( $X = \text{C}, \text{N}, \text{O}, \text{P}$ ) formation, carbon-carbon cleavage and carbon-hydrogen activation, all these photocatalytic reactions are limited to nonpolar solvent systems.<sup>30-33</sup> To broaden their applications in aqueous system, a prerequisite factor is to utilize water-stable MHPs. Ju *et al.* firstly extended the organic synthesis to aqueous solution with  $\text{DMASnI}_x\text{Br}_{3-x}$  for photoenzyme catalysis.<sup>279</sup> The nicotinamide adenine dinucleotide (NADH) yield was nearly 100% within only 30 min and exhibited stable reproducibility in four tests under blue LED irradiation (Fig. 13d).  $320 \mu\text{M}$  formic acid can be obtained over a period of 60 min in the photoenzymatic reaction, suggesting an efficient photocatalytic process in artificial photosynthesis.

## 4 Challenges and prospects

In this review, we summarize the significant advances in the development and applications of water-stable MHPs. To date, the water stability of MHPs has been achieved by surface engineering, common-ion effect and intrinsically stable MHPs. As

an emerging class of photocatalysts, the photocatalytic study of water-stable MHPs is still in their infancy. Several challenges and future research directions related to water-stable MHPs are identified as follows:

(1) Although various strategies have been proposed to obtain water stability of MHPs, to realize their photocatalytic applications, studies should be further focused on the charge carrier transport properties by exploring novel MHPs with intrinsic water compatibility (quasi-3D and 2D MHPs) and/or employing surface passivation that can protect MHPs from water while preserving good carrier transport features.<sup>318-323</sup> For example, constructing a MHP@shell core-shell heterostructure is a highly promising way to hit two birds with one stone. By bringing MHPs with semiconducting/conductive shell, not only new catalytically active sites<sup>324</sup> or protective coatings<sup>325</sup> can be introduced by the second phase, but more importantly rectifying interfaces may be obtained.

(2) While some water-stable MHP based photocatalytic systems have shown good photocatalytic activity in the degradation of organic dyes, more challenging and highly relevant fields such as hydrogen evolution and activation/valorization of  $\text{CO}_2$  are still in their early stages of development, and catalysts exhibit lower photocatalytic performance compared to traditional photocatalysts.<sup>326</sup> One possibility for the inferior activity might lie in the severe surface charge recombination.<sup>327</sup> In this regard, constructing a close-contact interface among MHP-based composites, which benefits the sufficient transfer and rectification of photogenerated charges, is highly desirable.<sup>328-330</sup> It has been proven that chemical modification or *in situ* synthesis can result in an intimate heterointerface.<sup>151,325,330,331</sup> Therefore, in the future, it is plausible to expect new avenues in this direction as well.

(3) Another vital direction of research is towards an in-depth understanding of reaction mechanisms over MHP-based photocatalysts, as the contemporary results are not entirely coherent and conclusive. Taking  $\text{CO}_2$  reduction reaction as an example, there are debates over the  $\text{CO}_2$  adsorption sites on bismuth-based  $\text{A}_3\text{Bi}_2\text{I}_9$  ( $A = \text{Rb}^+, \text{Cs}^+$  or  $\text{MA}^+$ )<sup>332-335</sup> and the origin of products (photocatalysis<sup>317</sup> or photolysis<sup>336,337</sup>). The photocatalytic HER reaction mechanism over  $\text{DMASnBr}_3$  is also not exhaustive. It is reported that the binding energy of electron polarons over  $\text{DMASnBr}_3$  surface dominates the HER activity, but the specific role of electron polarons, as driving force or trapping charges, needs further investigation.<sup>338</sup> In this regard, combining analytics, such as *in situ* Fourier-transform infrared spectroscopy, *in situ* Raman, *etc.*, with theoretical investigations, will provide new insights in understanding the mechanisms involved and thereby to the design of water-stable and efficient MHPs.

## Author contributions

H. Z.: conceptualization, formal analysis, investigation, writing – original draft; K. K.: supervision, funding acquisition, resources, writing – review & editing; S. O.: supervision, funding acquisition, resources, writing – review & editing.





## Conflicts of interest

There are no conflicts to declare.

## Acknowledgements

This work is supported by the Kvantum Institute Emerging Project (Charge carrier recombination dynamics in semiconductor materials) at the University of Oulu. H. Z. acknowledges the financial support of Tauno Tönning Foundation (grant no. 20210036) and University of Oulu Scholarship Fund (grant no. 20220010).

## Notes and references

- L. Gibson, E. N. Wilman and W. F. Laurance, *Trends Ecol. Evol.*, 2017, **32**, 922–935.
- N. Kannan and D. Vakeesan, *Renewable Sustainable Energy Rev.*, 2016, **62**, 1092–1105.
- J. H. Kim, D. Hansora, P. Sharma, J.-W. Jang and J. S. Lee, *Chem. Soc. Rev.*, 2019, **48**, 1908–1971.
- H. Nishiyama, T. Yamada, M. Nakabayashi, Y. Maehara, M. Yamaguchi, Y. Kuromiya, Y. Nagatsuma, H. Tokudome, S. Akiyama, T. Watanabe, R. Narushima, S. Okunaka, N. Shibata, T. Takata, T. Hisatomi and K. Domen, *Nature*, 2021, **598**, 304–307.
- P. Zhou, I. A. Navid, Y. Ma, Y. Xiao, P. Wang, Z. Ye, B. Zhou, K. Sun and Z. Mi, *Nature*, 2023, **613**, 66–70.
- B. A. Pinaud, J. D. Benck, L. C. Seitz, A. J. Forman, Z. Chen, T. G. Deutsch, B. D. James, K. N. Baum, G. N. Baum, S. Ardo, H. Wang, E. Miller and T. F. Jaramillo, *Energy Environ. Sci.*, 2013, **6**, 1983.
- Y.-H. Song, J. S. Yoo, E. K. Ji, C. W. Lee, G. S. Han, H. S. Jung and D.-H. Yoon, *Chem. Eng. J.*, 2016, **306**, 791–795.
- S. Chen, T. Takata and K. Domen, *Nat. Rev. Mater.*, 2017, **2**, 17050.
- N. A. Romero and D. A. Nicewicz, *Chem. Rev.*, 2016, **116**, 10075–10166.
- J. Twilton, C. Le, P. Zhang, M. H. Shaw, R. W. Evans and D. W. C. MacMillan, *Nat. Rev. Chem.*, 2017, **1**, 0052.
- J. Schneider, M. Matsuoka, M. Takeuchi, J. Zhang, Y. Horiuchi, M. Anpo and D. W. Bahnemann, *Chem. Rev.*, 2014, **114**, 9919–9986.
- Y. Ma, X. Wang, Y. Jia, X. Chen, H. Han and C. Li, *Chem. Rev.*, 2014, **114**, 9987–10043.
- G. Liao, Y. Gong, L. Zhang, H. Gao, G.-J. Yang and B. Fang, *Energy Environ. Sci.*, 2019, **12**, 2080–2147.
- A. Kumar Singh, C. Das and A. Indra, *Coord. Chem. Rev.*, 2022, **465**, 214516.
- V.-H. Nguyen, H. H. Do, T. Van Nguyen, P. Singh, P. Raizada, A. Sharma, S. S. Sana, A. N. Grace, M. Shokouhimehr, S. H. Ahn, C. Xia, S. Y. Kim and Q. Van Le, *Sol. Energy*, 2020, **211**, 584–599.
- A. Hossain, A. Bhattacharyya and O. Reiser, *Science*, 2019, **364**, eaav9713.
- F. E. Osterloh, *Chem. Mater.*, 2008, **20**, 35–54.
- K. Maeda and K. Domen, *J. Phys. Chem. Lett.*, 2010, **1**, 2655–2661.
- M. Rahman, H. Tian and T. Edvinsson, *Angew. Chem., Int. Ed.*, 2020, **59**, 16278–16293.
- A. Kojima, K. Teshima, Y. Shirai and T. Miyasaka, *J. Am. Chem. Soc.*, 2009, **131**, 6050–6051.
- H. Min, D. Y. Lee, J. Kim, G. Kim, K. S. Lee, J. Kim, M. J. Paik, Y. K. Kim, K. S. Kim, M. G. Kim, T. J. Shin and S. Il Seok, *Nature*, 2021, **598**, 444–450.
- G. Xing, N. Mathews, S. Sun, S. S. Lim, Y. M. Lam, M. Grätzel, S. Mhaisalkar and T. C. Sum, *Science*, 2013, **342**, 344–347.
- M. A. Green, A. Ho-Baillie and H. J. Snaith, *Nat. Photonics*, 2014, **8**, 506–514.
- Q. Dong, Y. Fang, Y. Shao, P. Mulligan, J. Qiu, L. Cao and J. Huang, *Science*, 2015, **347**, 967–970.
- C. Wehrenfennig, G. E. Eperon, M. B. Johnston, H. J. Snaith and L. M. Herz, *Adv. Mater.*, 2014, **26**, 1584–1589.
- P. Chen, W. Ong, Z. Shi, X. Zhao and N. Li, *Adv. Funct. Mater.*, 2020, **30**, 1909667.
- Y. Zhou and Y. Zhao, *Energy Environ. Sci.*, 2019, **12**, 1495–1511.
- S. Park, W. J. Chang, C. W. Lee, S. Park, H.-Y. Ahn and K. T. Nam, *Nat. Energy*, 2017, **2**, 16185.
- P. C. K. Vesborg, *Nat. Energy*, 2017, **2**, 16205.
- Y. Lin, J. Guo, J. San Martin, C. Han, R. Martinez and Y. Yan, *Chem. –Eur. J.*, 2020, **26**, 13118–13136.
- M. Corti, S. Bonomi, R. Chiara, L. Romani, P. Quadrelli and L. Malavasi, *Inorganics*, 2021, **9**, 56.
- M. Zhang, W. Sun, H. Lv and Z.-H. Zhang, *Curr. Opin. Green Sustainable Chem.*, 2021, **27**, 100390.
- V. Murugesu and S. P. Singh, *Chem. Rec.*, 2020, **20**, 1181–1197.
- S. Shyamal and N. Pradhan, *J. Phys. Chem. Lett.*, 2020, **11**, 6921–6934.
- S. Trivedi, D. Prochowicz, A. Kalam, M. M. Tavakoli and P. Yadav, *Renewable Sustainable Energy Rev.*, 2021, **145**, 111047.
- M. A. Raza, F. Li, M. Que, L. Zhu and X. Chen, *Mater. Adv.*, 2021, **2**, 7187–7209.
- X. Zhang, R. Tang, F. Li, R. Zheng and J. Huang, *Sol. RRL*, 2022, **6**, 2101058.
- J. Wang, Y. Shi, Y. Wang and Z. Li, *ACS Energy Lett.*, 2022, **7**, 2043–2059.
- C. B. Hiragond, N. S. Powar and S.-I. In, *Nanomaterials*, 2020, **10**, 2569.
- L. Romani and L. Malavasi, *ACS Omega*, 2020, **5**, 25511–25519.
- S. Purohit, K. L. Yadav and S. Satapathi, *Adv. Mater. Interfaces*, 2022, **9**, 2200058.
- V. Armenise, S. Colella, F. Fracassi and A. Listorti, *Nanomaterials*, 2021, **11**, 433.
- H. Huang, B. Pradhan, J. Hofkens, M. B. J. Roeffaers and J. A. Steele, *ACS Energy Lett.*, 2020, **5**, 1107–1123.
- J. Chen, C. Dong, H. Idriss, O. F. Mohammed and O. M. Bakr, *Adv. Energy Mater.*, 2020, **10**, 1902433.
- Y. Xu, M. Cao and S. Huang, *Nano Res.*, 2021, **14**, 3773–3794.



- 46 J. Luo, W. Zhang, H. Yang, Q. Fan, F. Xiong, S. Liu, D. Li and B. Liu, *EcoMat*, 2021, **3**, eom2.12079.
- 47 S. Pan, J. Li, Z. Wen, R. Lu, Q. Zhang, H. Jin, L. Zhang, Y. Chen and S. Wang, *Adv. Energy Mater.*, 2022, **12**, 2004002.
- 48 H. Zhou, Q. Chen, G. Li, S. Luo, T. B. Song, H. S. Duan, Z. Hong, J. You, Y. Liu and Y. Yang, *Science*, 2014, **345**, 542–546.
- 49 N. Tripathi, M. Yanagida, Y. Shirai, T. Masuda, L. Han and K. Miyano, *J. Mater. Chem. A*, 2015, **3**, 12081–12088.
- 50 W. Oh, S. Bae, S. Kim, N. Park, S.-I. Chan, H. Choi, H. Hwang and D. Kim, *Microelectron. Reliab.*, 2019, **100–101**, 113392.
- 51 C. Müller, T. Glaser, M. Plogmeyer, M. Sendner, S. Döring, A. A. Bakulin, C. Brzuska, R. Scheer, M. S. Pshenichnikov, W. Kowalsky, A. Pucci and R. Lovrinčić, *Chem. Mater.*, 2015, **27**, 7835–7841.
- 52 J. M. Frost, K. T. Butler, F. Brivio, C. H. Hendon, M. van Schilfgarde and A. Walsh, *Nano Lett.*, 2014, **14**, 2584–2590.
- 53 Y. Li, X. Xu, C. Wang, C. Wang, F. Xie, J. Yang and Y. Gao, *J. Phys. Chem. C*, 2015, **119**, 23996–24002.
- 54 E. Mosconi, J. M. Azpiroz and F. De Angelis, *Chem. Mater.*, 2015, **27**, 4885–4892.
- 55 A. M. A. Leguy, Y. Hu, M. Campoy-Quiles, M. I. Alonso, O. J. Weber, P. Azarhoosh, M. van Schilfgarde, M. T. Weller, T. Bein, J. Nelson, P. Docampo and P. R. F. Barnes, *Chem. Mater.*, 2015, **27**, 3397–3407.
- 56 J. Yang, B. D. Siempelkamp, D. Liu and T. L. Kelly, *ACS Nano*, 2015, **9**, 1955–1963.
- 57 Z. Song, A. Abate, S. C. Wathage, G. K. Liyanage, A. B. Phillips, U. Steiner, M. Graetzel and M. J. Heben, *Adv. Energy Mater.*, 2016, **6**, 1600846.
- 58 G. E. Eperon, S. N. Habisreutinger, T. Leijtens, B. J. Bruijnaers, J. J. van Franeker, D. W. DeQuilettes, S. Pathak, R. J. Sutton, G. Grancini, D. S. Ginger, R. A. J. Janssen, A. Petrozza and H. J. Snaith, *ACS Nano*, 2015, **9**, 9380–9393.
- 59 G. Grancini, V. D'Innocenzo, E. R. Dohner, N. Martino, A. R. Srimath Kandada, E. Mosconi, F. De Angelis, H. I. Karunadasa, E. T. Hoke and A. Petrozza, *Chem. Sci.*, 2015, **6**, 7305–7310.
- 60 C. Zheng and O. Rubel, *J. Phys. Chem. C*, 2019, **123**, 19385–19394.
- 61 S. Sun, D. Yuan, Y. Xu, A. Wang and Z. Deng, *ACS Nano*, 2016, **10**, 3648–3657.
- 62 H. Zhang, M. K. Nazeeruddin and W. C. H. Choy, *Adv. Mater.*, 2019, **31**, 1805702.
- 63 J. De Roo, M. Ibáñez, P. Geiregat, G. Nedelcu, W. Walravens, J. Maes, J. C. Martins, I. Van Driessche, M. V. Kovalenko and Z. Hens, *ACS Nano*, 2016, **10**, 2071–2081.
- 64 Y. Wei, Z. Cheng and J. Lin, *Chem. Soc. Rev.*, 2019, **48**, 310–350.
- 65 X. Du, R. Qiu, T. Zou, X. Chen, H. Chen and H. Zhou, *Adv. Mater. Interfaces*, 2019, **6**, 1900413.
- 66 A. Ciccioni, R. Panetta, A. Luongo, B. Brunetti, S. Vecchio Cipriotti, M. L. Mele and A. Latini, *Phys. Chem. Chem. Phys.*, 2019, **21**, 24768–24777.
- 67 B. Parida, I. S. Jin and J. W. Jung, *Chem. Mater.*, 2021, **33**, 5850–5858.
- 68 Y. Miao, M. Zheng, H. Wang, C. Chen, X. Ding, C. Wu, B. Wang, M. Zhai, X. Yang and M. Cheng, *J. Power Sources*, 2021, **492**, 229621.
- 69 I. Poli, S. Eslava and P. Cameron, *J. Mater. Chem. A*, 2017, **5**, 22325–22333.
- 70 Z. Xu, R. Chen, Y. Wu, R. He, J. Yin, W. Lin, B. Wu, J. Li and N. Zheng, *J. Mater. Chem. A*, 2019, **7**, 26849–26857.
- 71 S. Yang, Y. Wang, P. Liu, Y.-B. Cheng, H. J. Zhao and H. G. Yang, *Nat. Energy*, 2016, **1**, 15016.
- 72 Y. Guo, S. Apergi, N. Li, M. Chen, C. Yin, Z. Yuan, F. Gao, F. Xie, G. Brocks, S. Tao and N. Zhao, *Nat. Commun.*, 2021, **12**, 644.
- 73 S. Sasmal, S. Valiyaveetil, A. P. Upadhyay, R. G. S. Pala, S. Sivakumar, C. S. Sundar and D. Sornadurai, *MRS Commun.*, 2018, **8**, 289–296.
- 74 M. Aamir, A. F. Butt, M. D. Khan, M. Sher, A. Iqbal, M. A. Malik, U. Jabeen and J. Akhtar, *Optik*, 2020, **207**, 163828.
- 75 X. Liu, X. Wang, T. Zhang, Y. Miao, Z. Qin, Y. Chen and Y. Zhao, *Angew. Chem., Int. Ed.*, 2021, **60**, 12351–12355.
- 76 H. Wang, Z. Zhang, J. V. Milić, L. Tan, Z. Wang, R. Chen, X. Jing, C. Yi, Y. Ding, Y. Li, Y. Zhao, X. Zhang, A. Hagfeldt, M. Grätzel and J. Luo, *Adv. Energy Mater.*, 2021, **11**, 2101082.
- 77 Q. A. Akkerman, G. Rainò, M. V. Kovalenko and L. Manna, *Nat. Mater.*, 2018, **17**, 394–405.
- 78 H. Huang, B. Chen, Z. Wang, T. F. Hung, A. S. Sussha, H. Zhong and A. L. Rogach, *Chem. Sci.*, 2016, **7**, 5699–5703.
- 79 H. Wu, S. Lin, R. Wang, X. You and Y. Chi, *Nanoscale*, 2019, **11**, 5557–5563.
- 80 S. Liu, L. Yuan, Y. Zhao, Y. Chen, W. Xiang and X. Liang, *J. Alloys Compd.*, 2019, **806**, 1022–1028.
- 81 C.-H. Lu, S.-W. Kuo, C.-F. Huang and F.-C. Chang, *J. Phys. Chem. C*, 2009, **113**, 3517–3524.
- 82 B. P. Kennedy and A. B. P. Lever, *Can. J. Chem.*, 1972, **50**, 3488–3507.
- 83 H. Plenio, *ChemBioChem*, 2004, **5**, 650–655.
- 84 C. J. Drummond, G. Georgaklis and D. Y. C. Chan, *Langmuir*, 1996, **12**, 2617–2621.
- 85 K. C. Hoang and S. Mecozzi, *Langmuir*, 2004, **20**, 7347–7350.
- 86 Z. Li, Q. Hu, Z. Tan, Y. Yang, M. Leng, X. Liu, C. Ge, G. Niu and J. Tang, *ACS Appl. Mater. Interfaces*, 2018, **10**, 43915–43922.
- 87 Y. Mu, W. Zhang, X. Guo, G. Dong, M. Zhang and T. Lu, *ChemSusChem*, 2019, **12**, 4769–4774.
- 88 L. Yang, T. Wang, Q. Min, B. Liu, Z. Liu, X. Fan, J. Qiu, X. Xu, J. Yu and X. Yu, *ACS Omega*, 2019, **4**, 6084–6091.
- 89 A. Gericke and H. Hühnerfuss, *Thin Solid Films*, 1994, **245**, 74–82.
- 90 T. Lu, Y. Zhu, Y. Kang, J. Xu and A. Wang, *Int. J. Biol. Macromol.*, 2021, **193**, 1676–1684.
- 91 Y. Chang, Y. J. Yoon, G. Li, E. Xu, S. Yu, C.-H. Lu, Z. Wang, Y. He, C. H. Lin, B. K. Wagner, V. V. Tsukruk, Z. Kang, N. Thadhani, Y. Jiang and Z. Lin, *ACS Appl. Mater. Interfaces*, 2018, **10**, 37267–37276.



- 92 B. Shu, Y. Chang, L. Dong, L. Chen, H. Wang, S. Yang, J. Zhang, X. Cheng and D. Yu, *J. Lumin.*, 2021, **234**, 117962.
- 93 C. G. Sanjayan, M. S. Jyothi, M. Sakar and R. G. Balakrishna, *J. Colloid Interface Sci.*, 2021, **603**, 758–770.
- 94 L. Gomez, C. de Weerd, J. L. Hueso and T. Gregorkiewicz, *Nanoscale*, 2017, **9**, 631–636.
- 95 A. Jana, K. N. Lawrence, M. B. Teunis, M. Mandal, A. Kumbhar and R. Sardar, *Chem. Mater.*, 2016, **28**, 1107–1120.
- 96 S. Biswas, S. Akhil, N. Kumar, M. Palabathuni, R. Singh, V. G. V. Dutt and N. Mishra, *J. Phys. Chem. Lett.*, 2023, **14**, 1910–1917.
- 97 Z. Chen, Y. Hu, J. Wang, Q. Shen, Y. Zhang, C. Ding, Y. Bai, G. Jiang, Z. Li and N. Gaponik, *Chem. Mater.*, 2020, **32**, 1517–1525.
- 98 J.-C. Wang, N. Li, A. M. Idris, J. Wang, X. Du, Z. Pan and Z. Li, *Sol. RRL*, 2021, **5**, 1–8.
- 99 J. G. Smith and P. K. Jain, *J. Am. Chem. Soc.*, 2016, **138**, 6765–6773.
- 100 Y. Yuan, H. Zhu, K. Hills-Kimball, T. Cai, W. Shi, Z. Wei, H. Yang, Y. Candler, P. Wang, J. He and O. Chen, *Angew. Chem., Int. Ed.*, 2020, **59**, 22563–22569.
- 101 M. Zhao, D. Ding, F. Yang, D. Wang, J. Lv, W. Hu, C. Lu and Z. Tang, *Nano Res.*, 2017, **10**, 1249–1257.
- 102 J. Chang, Y. Ogomi, C. Ding, Y. H. Zhang, T. Toyoda, S. Hayase, K. Katayama and Q. Shen, *Phys. Chem. Chem. Phys.*, 2017, **19**, 6358–6367.
- 103 H. Lu, X. Zhu, C. Miller, J. San Martin, X. Chen, E. M. Miller, Y. Yan and M. C. Beard, *J. Chem. Phys.*, 2019, **151**, 204305.
- 104 J. Pan, Y. Shang, J. Yin, M. De Bastiani, W. Peng, I. Dursun, L. Sinatra, A. M. El-Zohry, M. N. Hedhili, A.-H. Emwas, O. F. Mohammed, Z. Ning and O. M. Bakr, *J. Am. Chem. Soc.*, 2018, **140**, 562–565.
- 105 S. Han, H. Zhang, R. Wang and Q. He, *Mater. Sci. Semicond. Process.*, 2021, **131**, 105847.
- 106 C. Lin, J. Li, N. She, S. Huang, C. Huang, I. Wang, F. Tsai, C. Wei, T. Lee, D. Wang, C. Wen, S. Li, A. Yabushita, C. Luo, C. Chen and C. Chen, *Small*, 2022, **18**, 2107881.
- 107 C. Gao, F. Zhang, X. Gu, J. Huang, K. Wang, S. Zhang, S. Liu and Q. Tian, *ACS Appl. Energy Mater.*, 2021, **4**, 4021–4028.
- 108 C. Zhao, Z. He, P. Wangyang, J. Tan, C. Shi, A. Pan, L. He and Y. Liu, *ACS Appl. Nano Mater.*, 2022, **5**, 13737–13744.
- 109 J. Chen, S.-G. Kim, X. Ren, H. S. Jung and N.-G. Park, *J. Mater. Chem. A*, 2019, **7**, 4977–4987.
- 110 W. Zhang, Q. Li and Z. Li, *Adv. Mater. Interfaces*, 2022, **9**, 2101881.
- 111 H. Zhang, Y. Wu, C. Shen, E. Li, C. Yan, W. Zhang, H. Tian, L. Han and W. Zhu, *Adv. Energy Mater.*, 2019, **9**, 1803573.
- 112 Y. Yang, J. Liang, Z. Zhang, C. Tian, X. Wu, Y. Zheng, Y. Huang, J. Wang, Z. Zhou, M. He, Z. Chen and C. Chen, *ChemSusChem*, 2022, **15**, e202102474.
- 113 Y. Li, M. Cai, M. Shen, Y. Cai and R.-J. Xie, *J. Mater. Chem. C*, 2022, **10**, 8356–8363.
- 114 Q. Chen, X. Yang, Y. Zhou and B. Song, *New J. Chem.*, 2021, **45**, 15118–15130.
- 115 H. Wu, S. Wang, F. Cao, J. Zhou, Q. Wu, H. Wang, X. Li, L. Yin and X. Yang, *Chem. Mater.*, 2019, **31**, 1936–1940.
- 116 A. F. Carrizo, G. K. Belmonte, F. S. Santos, C. W. Backes, G. B. Strapasson, L. C. Schmidt, F. S. Rodembusch and D. E. Weibel, *ACS Appl. Mater. Interfaces*, 2021, **13**, 59252–59262.
- 117 B. Yu, S. Liang, F. Zhang, Z. Li, B. Liu and X. Ding, *Photonics Res.*, 2021, **9**, 1559.
- 118 S. Wang, Z. Zhang, Z. Tang, C. Su, W. Huang, Y. Li and G. Xing, *Nano Energy*, 2021, **82**, 105712.
- 119 Y. Yang and H. Zhao, *Appl. Surf. Sci.*, 2022, **577**, 151895.
- 120 J. Han, M. Sharipov, S. Hwang, Y. Lee, B. T. Huy and Y.-I. Lee, *Sci. Rep.*, 2022, **12**, 3147.
- 121 H. C. Yoon, H. Kang, S. Lee, J. H. Oh, H. Yang and Y. R. Do, *ACS Appl. Mater. Interfaces*, 2016, **8**, 18189–18200.
- 122 J. Ren, X. Dong, G. Zhang, T. Li and Y. Wang, *New J. Chem.*, 2017, **41**, 13961–13967.
- 123 Y. Zhang, B. Zhang, Y. Fu, Y. Han, T. Zhang, L. Zhang, J. Guo and X. Zhang, *J. Mater. Chem. C*, 2022, **10**, 8609–8616.
- 124 H. Wang, H. Lin, X. Piao, P. Tian, M. Fang, X. An, C. Luo, R. Qi, Y. Chen and H. Peng, *J. Mater. Chem. C*, 2017, **5**, 12044–12049.
- 125 S. Kango, S. Kalia, A. Celli, J. Njuguna, Y. Habibi and R. Kumar, *Prog. Polym. Sci.*, 2013, **38**, 1232–1261.
- 126 S. Masi, A. Rizzo, F. Aiello, F. Balzano, G. Uccello-Barretta, A. Listorti, G. Gigli and S. Colella, *Nanoscale*, 2015, **7**, 18956–18963.
- 127 B. Erman and P. J. Flory, *Macromolecules*, 1986, **19**, 2342–2353.
- 128 C. Carrillo-Carrión, P. del Pino and B. Pelaz, *Appl. Mater. Today*, 2019, **15**, 562–569.
- 129 Y. Wang, J. He, H. Chen, J. Chen, R. Zhu, P. Ma, A. Towers, Y. Lin, A. J. Gesquiere, S. Wu and Y. Dong, *Adv. Mater.*, 2016, **28**, 10710–10717.
- 130 Y. Wei, X. Deng, Z. Xie, X. Cai, S. Liang, P. Ma, Z. Hou, Z. Cheng and J. Lin, *Adv. Funct. Mater.*, 2017, **27**, 1703535.
- 131 J. An, M. Chen, G. Liu, Y. Hu, R. Chen, Y. Lyu, S. Sharma and Y. Liu, *Anal. Bioanal. Chem.*, 2021, **413**, 1739–1747.
- 132 Y. Xin, H. Zhao and J. Zhang, *ACS Appl. Mater. Interfaces*, 2018, **10**, 4971–4980.
- 133 H. Sun, Z. Yang, M. Wei, W. Sun, X. Li, S. Ye, Y. Zhao, H. Tan, E. L. Kynaston, T. B. Schon, H. Yan, Z.-H. Lu, G. A. Ozin, E. H. Sargent and D. S. Seferos, *Adv. Mater.*, 2017, **29**, 1701153.
- 134 V. A. Hintermayr, C. Lampe, M. Löw, J. Roemer, W. Vanderlinden, M. Gramlich, A. X. Böhm, C. Sattler, B. Nickel, T. Lohmüller and A. S. Urban, *Nano Lett.*, 2019, **19**, 4928–4933.
- 135 J. Zhang, P. Jiang, Y. Wang, X. Liu, J. Ma and G. Tu, *ACS Appl. Mater. Interfaces*, 2020, **12**, 3080–3085.
- 136 Q. Zhou, Z. Bai, W. Lu, Y. Wang, B. Zou and H. Zhong, *Adv. Mater.*, 2016, **28**, 9163–9168.
- 137 G. Jiang, C. Guhrenz, A. Kirch, L. Sonntag, C. Bauer, X. Fan, J. Wang, S. Reineke, N. Gaponik and A. Eychmüller, *ACS Nano*, 2019, **13**, 10386–10396.
- 138 Z. Lu, Y. Li, Y. Xue, W. Zhou, S. Bayer, I. D. Williams, A. L. Rogach and S. Nagl, *ACS Appl. Nano Mater.*, 2022, **5**, 5025–5034.



- 139 Y. Shu, Y. Wang, J. Guan, Z. Ji, Q. Xu and X. Hu, *Anal. Chem.*, 2022, **94**, 5415–5424.
- 140 H. Zhang, X. Wang, Q. Liao, Z. Xu, H. Li, L. Zheng and H. Fu, *Adv. Funct. Mater.*, 2017, **27**, 1604382.
- 141 J. Hai, H. Li, Y. Zhao, F. Chen, Y. Peng and B. Wang, *Chem. Commun.*, 2017, **53**, 5400–5403.
- 142 A. Pramanik, K. Gates, S. Patibandla, D. Davis, S. Begum, R. Iftekhar, S. Alamgir, S. Paige, M. M. Porter and P. C. Ray, *ACS Appl. Bio Mater.*, 2019, **2**, 5872–5879.
- 143 S. N. Raja, Y. Bekenstein, M. A. Koc, S. Fischer, D. Zhang, L. Lin, R. O. Ritchie, P. Yang and A. P. Alivisatos, *ACS Appl. Mater. Interfaces*, 2016, **8**, 35523–35533.
- 144 J. Xi, Y. Wu, W. Chen, Q. Li, J. Li, Y. Shen, H. Chen, G. Xu, H. Yang, Z. Chen, N. Li, J. Zhu, Y. Li and Y. Li, *Nano Energy*, 2022, **93**, 106846.
- 145 Z. Zhang, L. Liu, H. Huang, L. Li, Y. Wang, J. Xu and J. Xu, *Appl. Surf. Sci.*, 2020, **526**, 146735.
- 146 Z. Zhang, L. Li, L. Liu, X. Xiao, H. Huang and J. Xu, *J. Phys. Chem. C*, 2020, **124**, 22228–22234.
- 147 F.-J. Kahle, C. Saller, A. Köhler and P. Strohhriegl, *Adv. Energy Mater.*, 2017, **7**, 1700306.
- 148 T. Xu, J. Stevens, J. A. Villa, J. T. Goldbach, K. W. Guarini, C. T. Black, C. J. Hawker and T. P. Russell, *Adv. Funct. Mater.*, 2003, **13**, 698–702.
- 149 Y. Liu, Z. Wang, S. Liang, Z. Li, M. Zhang, H. Li and Z. Lin, *Nano Lett.*, 2019, **19**, 9019–9028.
- 150 K. Manokruang and E. Manias, *Mater. Lett.*, 2009, **63**, 1144–1147.
- 151 W. Hu, Z. Wen, X. Yu, P. Qian, W. Lian, X. Li, Y. Shang, X. Wu, T. Chen, Y. Lu, M. Wang and S. Yang, *Adv. Sci.*, 2021, **8**, 2004662.
- 152 F. Wang, M. Endo, S. Mouri, Y. Miyauchi, Y. Ohno, A. Wakamiya, Y. Murata and K. Matsuda, *Nanoscale*, 2016, **8**, 11882–11888.
- 153 S. Kundu and T. L. Kelly, *Mater. Chem. Front.*, 2018, **2**, 81–89.
- 154 C. Wu, K. Wang, Y. Yan, D. Yang, Y. Jiang, B. Chi, J. Liu, A. R. Esker, J. Rowe, A. J. Morris, M. Sanghadasa and S. Priya, *Adv. Funct. Mater.*, 2019, **29**, 1804419.
- 155 M. Meyns, M. Perálvarez, A. Heuer-Jungemann, W. Hertog, M. Ibáñez, R. Nafria, A. Genç, J. Arbiol, M. V. Kovalenko, J. Carreras, A. Cabot and A. G. Kanaras, *ACS Appl. Mater. Interfaces*, 2016, **8**, 19579–19586.
- 156 A. F. Demirörs, A. van Blaaderen and A. Imhof, *Langmuir*, 2010, **26**, 9297–9303.
- 157 A. Loiudice, S. Saris, E. Oveisi, D. T. L. Alexander and R. Buonsanti, *Angew. Chem., Int. Ed.*, 2017, **56**, 10696–10701.
- 158 H. Yu, X. Xu, H. Liu, Y. Wan, X. Cheng, J. Chen, Y. Ye and L. Dai, *ACS Nano*, 2020, **14**, 552–558.
- 159 H. Hu, L. Wu, Y. Tan, Q. Zhong, M. Chen, Y. Qiu, D. Yang, B. Sun, Q. Zhang and Y. Yin, *J. Am. Chem. Soc.*, 2018, **140**, 406–412.
- 160 H. Liu, Y. Tan, M. Cao, H. Hu, L. Wu, X. Yu, L. Wang, B. Sun and Q. Zhang, *ACS Nano*, 2019, **13**, 5366–5374.
- 161 Q. Zhong, M. Cao, H. Hu, D. Yang, M. Chen, P. Li, L. Wu and Q. Zhang, *ACS Nano*, 2018, **12**, 8579–8587.
- 162 Y.-T. Hsieh, Y.-F. Lin and W.-R. Liu, *ACS Appl. Mater. Interfaces*, 2020, **12**, 58049–58059.
- 163 Z. Li, C. Song, J. Li, G. Liang, L. Rao, S. Yu, X. Ding, Y. Tang, B. Yu, J. Ou, U. Lemmer and G. Gomard, *Adv. Mater. Technol.*, 2020, **5**, 1900941.
- 164 P. M. Talianov, O. O. Peltek, M. Masharin, S. Khubezhov, M. A. Baranov, A. Drabavičius, A. S. Timin, L. E. Zelenkov, A. P. Pushkarev, S. V. Makarov and M. V. Zyuzin, *J. Phys. Chem. Lett.*, 2021, **12**, 8991–8998.
- 165 F. Gao, W. Yang, X. Liu, Y. Li, W. Liu, H. Xu and Y. Liu, *Chem. Eng. J.*, 2021, **407**, 128001.
- 166 H. Wu, Y. Chen, W. Zhang, M. S. Khan and Y. Chi, *ACS Appl. Nano Mater.*, 2021, **4**, 11791–11800.
- 167 S. Li, D. Lei, W. Ren, X. Guo, S. Wu, Y. Zhu, A. L. Rogach, M. Chhowalla and A. K. Y. Jen, *Nat. Commun.*, 2020, **11**, 1192.
- 168 C.-Y. You, F.-M. Li, L.-H. Lin, J.-S. Lin, Q.-Q. Chen, P. M. Radjenovic, Z.-Q. Tian and J.-F. Li, *Nano Energy*, 2020, **71**, 104554.
- 169 Y. Huang, F. Li, L. Qiu, F. Lin, Z. Lai, S. Wang, L. Lin, Y. Zhu, Y. Wang, Y. Jiang and X. Chen, *ACS Appl. Mater. Interfaces*, 2019, **11**, 26384–26391.
- 170 Z. Zheng, L. Liu, F. Yi and J. Zhao, *J. Lumin.*, 2019, **216**, 116722.
- 171 K. K. Chan, D. Giovanni, H. He, T. C. Sum and K.-T. Yong, *ACS Appl. Nano Mater.*, 2021, **4**, 9022–9033.
- 172 K. K. Chan, S. H. K. Yap, D. Giovanni, T. C. Sum and K.-T. Yong, *Microchem. J.*, 2022, **180**, 107624.
- 173 M. He, Y. Cheng, L. Shen, C. Shen, H. Zhang, W. Xiang and X. Liang, *Appl. Surf. Sci.*, 2018, **448**, 400–406.
- 174 J. Y. Kim, K. I. Shim, J. W. Han, J. Joo, N. H. Heo and K. Seff, *Adv. Mater.*, 2020, **32**, 2001868.
- 175 Y. Zhang, L. Han, B. Li and Y. Xu, *Chem. Eng. J.*, 2022, **437**, 135290.
- 176 J. Jiang, G. Shao, Z. Zhang, L. Ding, H. Zhang, J. Liu, Z. Chen, W. Xiang and X. Liang, *Chem. Commun.*, 2018, **54**, 12302–12305.
- 177 C. Shen, Y. Zhao, L. Yuan, L. Ding, Y. Chen, H. Yang, S. Liu, J. Nie, W. Xiang and X. Liang, *Chem. Eng. J.*, 2020, **382**, 122868.
- 178 S. Yuan, D. Chen, X. Li, J. Zhong and X. Xu, *ACS Appl. Mater. Interfaces*, 2018, **10**, 18918–18926.
- 179 P. Song, B. Qiao, D. Song, J. Cao, Z. Shen, G. Zhang, Z. Xu, S. Zhao, S. Wageh and A. Al-Ghamdi, *J. Mater. Sci.*, 2020, **55**, 9739–9747.
- 180 Z. Tan, Y. Chu, J. Chen, J. Li, G. Ji, G. Niu, L. Gao, Z. Xiao and J. Tang, *Adv. Mater.*, 2020, **32**, 2002443.
- 181 Z. Li, E. Hofman, J. Li, A. H. Davis, C.-H. Tung, L.-Z. Wu and W. Zheng, *Adv. Funct. Mater.*, 2018, **28**, 1704288.
- 182 Y. You, W. Tian, M. Wang, F. Cao, H. Sun and L. Li, *Adv. Mater. Interfaces*, 2020, **7**, 2000537.
- 183 G. Kang, H. Lee, J. Moon, H.-S. Jang, D.-H. Cho and D. Byun, *ACS Appl. Nano Mater.*, 2022, **5**, 6726–6735.
- 184 Q. Wang, Q. Dong, T. Li, A. Gruverman and J. Huang, *Adv. Mater.*, 2016, **28**, 6734–6739.
- 185 J. Zeng, C. Meng, X. Li, Y. Wu, S. Liu, H. Zhou, H. Wang and H. Zeng, *Adv. Funct. Mater.*, 2019, **29**, 1904461.



- 186 A. Pron and P. Rannou, *Prog. Polym. Sci.*, 2002, **27**, 135–190.
- 187 Y. Li and R. Qian, *Synth. Met.*, 1993, **53**, 149–154.
- 188 R. Ansari, *E-J. Chem.*, 2006, **3**, 186–201.
- 189 M. D. Groner, S. M. George, R. S. McLean and P. F. Carcia, *Appl. Phys. Lett.*, 2006, **88**, 051907.
- 190 G. Li, F. W. R. Rivarola, N. J. L. K. Davis, S. Bai, T. C. Jellicoe, F. de la Peña, S. Hou, C. Ducati, F. Gao, R. H. Friend, N. C. Greenham and Z.-K. Tan, *Adv. Mater.*, 2016, **28**, 3528–3534.
- 191 R. W. Johnson, A. Hultqvist and S. F. Bent, *Mater. Today*, 2014, **17**, 236–246.
- 192 C.-C. Shih, P.-C. Chen, G.-L. Lin, C.-W. Wang and H.-T. Chang, *ACS Nano*, 2015, **9**, 312–319.
- 193 S. Liu and M.-Y. Han, *Chem.-Asian J.*, 2009, **5**, 36–45.
- 194 A. Soleimani Dorcheh and M. H. Abbasi, *J. Mater. Process. Technol.*, 2008, **199**, 10–26.
- 195 H.-C. Wang, S.-Y. Lin, A.-C. Tang, B. P. Singh, H.-C. Tong, C.-Y. Chen, Y.-C. Lee, T.-L. Tsai and R.-S. Liu, *Angew. Chem., Int. Ed.*, 2016, **55**, 7924–7929.
- 196 M. Liu, S. Wang and L. Jiang, *Nat. Rev. Mater.*, 2017, **2**, 17036.
- 197 S. Wang, H. Wang, D. Zhang, Y. Dou, W. Li, F. Cao, L. Yin, L. Wang, Z.-J. Zhang, J. Zhang and X. Yang, *Chem. Eng. J.*, 2022, **437**, 135303.
- 198 X. Tian, T. Verho and R. H. A. Ras, *Science*, 2016, **352**, 142–143.
- 199 D. K. Sharma, S. Hirata and M. Vacha, *Nat. Commun.*, 2019, **10**, 4499.
- 200 R. H. Baney, M. Itoh, A. Sakakibara and T. Suzuki, *Chem. Rev.*, 1995, **95**, 1409–1430.
- 201 J. M. Newsam, *Science*, 1986, **231**, 1093–1099.
- 202 Y. Li and J. Yu, *Chem. Rev.*, 2014, **114**, 7268–7316.
- 203 V. Van Speybroeck, K. Hemelsoet, L. Joos, M. Waroquier, R. G. Bell and C. R. A. Catlow, *Chem. Soc. Rev.*, 2015, **44**, 7044–7111.
- 204 J.-Y. Sun, F. T. Rabouw, X.-F. Yang, X.-Y. Huang, X.-P. Jing, S. Ye and Q.-Y. Zhang, *Adv. Funct. Mater.*, 2017, **27**, 1704371.
- 205 G. Tong, W. Song, L. K. Ono and Y. Qi, *Appl. Phys. Lett.*, 2022, **120**, 161604.
- 206 J.-F. Liao, Y.-F. Xu, X.-D. Wang, H.-Y. Chen and D.-B. Kuang, *ACS Appl. Mater. Interfaces*, 2018, **10**, 42301–42309.
- 207 Y. Xu, X. Wang, J. Liao, B. Chen, H. Chen and D. Kuang, *Adv. Mater. Interfaces*, 2018, **5**, 1801015.
- 208 Y. Liu, Z. Yang, D. Cui, X. Ren, J. Sun, X. Liu, J. Zhang, Q. Wei, H. Fan, F. Yu, X. Zhang, C. Zhao and S. F. Liu, *Adv. Mater.*, 2015, **27**, 5176–5183.
- 209 H. Yin, J. Chen, P. Guan, D. Zheng, Q. Kong, S. Yang, P. Zhou, B. Yang, T. Pullerits and K. Han, *Angew. Chem., Int. Ed.*, 2021, **60**, 22693–22699.
- 210 S. Wang and X. Wang, *Small*, 2015, **11**, 3097–3112.
- 211 W. Lu, Z. Wei, Z.-Y. Gu, T.-F. Liu, J. Park, J. Park, J. Tian, M. Zhang, Q. Zhang, T. Gentle III, M. Bosch and H.-C. Zhou, *Chem. Soc. Rev.*, 2014, **43**, 5561–5593.
- 212 W. Nie and H. Tsai, *J. Mater. Chem. A*, 2022, **10**, 19518–19533.
- 213 D. Zhang, Y. Xu, Q. Liu and Z. Xia, *Inorg. Chem.*, 2018, **57**, 4613–4619.
- 214 G. Lu, S. Li, Z. Guo, O. K. Farha, B. G. Hauser, X. Qi, Y. Wang, X. Wang, S. Han, X. Liu, J. S. DuChene, H. Zhang, Q. Zhang, X. Chen, J. Ma, S. C. J. Loo, W. D. Wei, Y. Yang, J. T. Hupp and F. Huo, *Nat. Chem.*, 2012, **4**, 310–316.
- 215 S. Mollick, T. N. Mandal, A. Jana, S. Fajal, A. V. Desai and S. K. Ghosh, *ACS Appl. Nano Mater.*, 2019, **2**, 1333–1340.
- 216 S. Ahmed, S. Lahkar, S. Doley, D. Mohanta and S. Kumar Dolui, *J. Photochem. Photobiol., A*, 2023, **443**, 114821.
- 217 G.-Y. Qiao, D. Guan, S. Yuan, H. Rao, X. Chen, J.-A. Wang, J.-S. Qin, J.-J. Xu and J. Yu, *J. Am. Chem. Soc.*, 2021, **143**, 14253–14260.
- 218 Z. Xia, B. Shi, W. Zhu, Y. Xiao and C. Lü, *Adv. Funct. Mater.*, 2022, **32**, 2207655.
- 219 J. Hou, P. Chen, A. Shukla, A. Krajnc, T. Wang, X. Li, R. Doasa, L. H. G. Tizei, B. Chan, D. N. Johnstone, R. Lin, T. U. Schüllli, I. Martens, D. Appadoo, M. S. Ari, Z. Wang, T. Wei, S. Lo, M. Lu, S. Li, E. B. Namdas, G. Mali, A. K. Cheetham, S. M. Collins, V. Chen, L. Wang and T. D. Bennett, *Science*, 2021, **374**, 621–625.
- 220 T. D. Bennett, Y. Yue, P. Li, A. Qiao, H. Tao, N. G. Greaves, T. Richards, G. I. Lampronti, S. A. T. Redfern, F. Blanc, O. K. Farha, J. T. Hupp, A. K. Cheetham and D. A. Keen, *J. Am. Chem. Soc.*, 2016, **138**, 3484–3492.
- 221 S. Horike, S. Shimomura and S. Kitagawa, *Nat. Chem.*, 2009, **1**, 695–704.
- 222 Y. Chen, Z. Lai, X. Zhang, Z. Fan, Q. He, C. Tan and H. Zhang, *Nat. Rev. Chem*, 2020, **4**, 243–256.
- 223 R. Kappera, D. Voiry, S. E. Yalcin, B. Branch, G. Gupta, A. D. Mohite and M. Chhowalla, *Nat. Mater.*, 2014, **13**, 1128–1134.
- 224 D. Voiry, A. Mohite and M. Chhowalla, *Chem. Soc. Rev.*, 2015, **44**, 2702–2712.
- 225 S. Caicedo-Dávila, H. Funk, R. Lovrinčić, C. Müller, M. Sendner, O. Cojocar-Mirédin, F. Lehmann, R. Gunder, A. Franz, S. Levenco, A. V. Cohen, L. Kronik, B. Haas, C. T. Koch and D. Abou-Ras, *J. Phys. Chem. C*, 2019, **123**, 17666–17677.
- 226 J. Hui, Y. Jiang, Ö. Ö. Gökçinar, J. Tang, Q. Yu, M. Zhang and K. Yu, *Chem. Mater.*, 2020, **32**, 4574–4583.
- 227 M. I. Saidaminov, M. A. Haque, J. Almutlaq, S. Sarmah, X.-H. Miao, R. Begum, A. A. Zhumekenov, I. Dursun, N. Cho, B. Murali, O. F. Mohammed, T. Wu and O. M. Bakr, *Adv. Opt. Mater.*, 2017, **5**, 1600704.
- 228 C. de Weerd, J. Lin, L. Gomez, Y. Fujiwara, K. Suenaga and T. Gregorkiewicz, *J. Phys. Chem. C*, 2017, **121**, 19490–19496.
- 229 I. Dursun, M. De Bastiani, B. Turedi, B. Alamer, A. Shkurenko, J. Yin, A. M. El-Zohry, I. Gereige, A. AlSaggaf, O. F. Mohammed, M. Eddaoudi and O. M. Bakr, *ChemSusChem*, 2017, **10**, 3746–3749.
- 230 M. I. Saidaminov, J. Almutlaq, S. Sarmah, I. Dursun, A. A. Zhumekenov, R. Begum, J. Pan, N. Cho, O. F. Mohammed and O. M. Bakr, *ACS Energy Lett.*, 2016, **1**, 840–845.
- 231 Q. A. Akkerman, T. P. T. Nguyen, S. C. Boehme, F. Montanarella, D. N. Dirin, P. Wechsler, F. Beiglböck,



- G. Rainò, R. Erni, C. Katan, J. Even and M. V. Kovalenko, *Science*, 2022, **3616**, 1–13.
- 232 X. Zhang, B. Xu, J. Zhang, Y. Gao, Y. Zheng, K. Wang and X. W. Sun, *Adv. Funct. Mater.*, 2016, **26**, 4595–4600.
- 233 J. Xu, W. Huang, P. Li, D. R. Onken, C. Dun, Y. Guo, K. B. Ucer, C. Lu, H. Wang, S. M. Geyer, R. T. Williams and D. L. Carroll, *Adv. Mater.*, 2017, **29**, 1703703.
- 234 B. Qiao, P. Song, J. Cao, S. Zhao, Z. Shen, D. Gao, Z. Liang, Z. Xu, D. Song and X. Xu, *Nanotechnology*, 2017, **28**, 445602.
- 235 X. Tang, Z. Hu, W. Yuan, W. Hu, H. Shao, D. Han, J. Zheng, J. Hao, Z. Zang, J. Du, Y. Leng, L. Fang and M. Zhou, *Adv. Opt. Mater.*, 2017, **5**, 1600788.
- 236 Z. Ma, F. Li, G. Qi, L. Wang, C. Liu, K. Wang, G. Xiao and B. Zou, *Nanoscale*, 2019, **11**, 820–825.
- 237 J. Deng, J. Xun, W. Shen, M. Li and R. He, *Mater. Res. Bull.*, 2021, **140**, 111296.
- 238 X. Zhang, H. Wang, Y. Hu, Y. Pei, S. Wang, Z. Shi, V. L. Colvin, S. Wang, Y. Zhang and W. W. Yu, *J. Phys. Chem. Lett.*, 2019, **10**, 1750–1756.
- 239 J. P. McKaveney and M. D. Buck, *Anal. Chem.*, 1974, **46**, 650–654.
- 240 B. Zhou, Z. Liu, H. Li, S. Fang, F. Fang, Y. Wang, F. Chen and Y. Shi, *Adv. Photonics Res.*, 2021, **2**, 2100143.
- 241 J. Li, Z. Tan, M. Hu, C. Chen, J. Luo, S. Li, L. Gao, Z. Xiao, G. Niu and J. Tang, *Front. Optoelectron.*, 2019, **12**, 352–364.
- 242 Q. Ba, J. Kim, H. Im, S. Lin and A. Jana, *J. Colloid Interface Sci.*, 2022, **606**, 808–816.
- 243 J. You, Y. Yang, Z. Hong, T.-B. Song, L. Meng, Y. Liu, C. Jiang, H. Zhou, W.-H. Chang, G. Li and Y. Yang, *Appl. Phys. Lett.*, 2014, **105**, 183902.
- 244 L. Wu, H. Hu, Y. Xu, S. Jiang, M. Chen, Q. Zhong, D. Yang, Q. Liu, Y. Zhao, B. Sun, Q. Zhang and Y. Yin, *Nano Lett.*, 2017, **17**, 5799–5804.
- 245 M. Xie, H. Liu, F. Chun, W. Deng, C. Luo, Z. Zhu, M. Yang, Y. Li, W. Li, W. Yan and W. Yang, *Small*, 2019, **15**, 1901994.
- 246 A. Pramanik, S. Patibandla, Y. Gao, K. Gates and P. C. Ray, *JACS Au*, 2021, **1**, 53–65.
- 247 Y. Liu, F. Li, Q. Liu and Z. Xia, *Chem. Mater.*, 2018, **30**, 6922–6929.
- 248 S. Mamgain, V. Kunnathodi and A. Yella, *Energy Technol.*, 2020, **8**, 1900890.
- 249 Q. Jing, M. Zhang, X. Huang, X. Ren, P. Wang and Z. Lu, *Nanoscale*, 2017, **9**, 7391–7396.
- 250 K. Chen, K. Qi, T. Zhou, T. Yang, Y. Zhang, Z. Guo, C.-K. Lim, J. Zhang, I. Žutić, H. Zhang and P. N. Prasad, *Nano-Micro Lett.*, 2021, **13**, 172.
- 251 J. Zhu, Y. Zhu, J. Huang, L. Hou, J. Shen and C. Li, *Nanoscale*, 2020, **12**, 11842–11846.
- 252 F. Fang, W. Chen, Y. Li, H. Liu, M. Mei, R. Zhang, J. Hao, M. Mikita, W. Cao, R. Pan, K. Wang and X. W. Sun, *Adv. Funct. Mater.*, 2018, **28**, 1706000.
- 253 X. Zhang, X. Bai, H. Wu, X. Zhang, C. Sun, Y. Zhang, W. Zhang, W. Zheng, W. W. Yu and A. L. Rogach, *Angew. Chem., Int. Ed.*, 2018, **57**, 3337–3342.
- 254 H. Jiang, Z. Yan, H. Zhao, S. Yuan, Z. Yang, J. Li, B. Liu, T. Niu, J. Feng, Q. Wang, D. Wang, H. Yang, Z. Liu and S. F. Liu, *ACS Appl. Energy Mater.*, 2018, **1**, 900–909.
- 255 L. N. Quan, M. Yuan, R. Comin, O. Voznyy, E. M. Beaugregard, S. Hoogland, A. Buin, A. R. Kirmani, K. Zhao, A. Amassian, D. H. Kim and E. H. Sargent, *J. Am. Chem. Soc.*, 2016, **138**, 2649–2655.
- 256 Y. Lin, Y. Bai, Y. Fang, Q. Wang, Y. Deng and J. Huang, *ACS Energy Lett.*, 2017, **2**, 1571–1572.
- 257 Y. Yang, C. Hou and T.-X. Liang, *Phys. Chem. Chem. Phys.*, 2021, **23**, 7145–7152.
- 258 D. Yoo, J. Y. Woo, Y. Kim, S. W. Kim, S.-H. Wei, S. Jeong and Y.-H. Kim, *J. Phys. Chem. Lett.*, 2020, **11**, 652–658.
- 259 A. Jana and K. S. Kim, *ACS Energy Lett.*, 2018, **3**, 2120–2126.
- 260 A. Jana and K. S. Kim, *ACS Appl. Energy Mater.*, 2019, **2**, 4496–4503.
- 261 K.-K. Liu, Q. Liu, D.-W. Yang, Y.-C. Liang, L.-Z. Sui, J.-Y. Wei, G.-W. Xue, W.-B. Zhao, X.-Y. Wu, L. Dong and C.-X. Shan, *Light: Sci. Appl.*, 2020, **9**, 44.
- 262 L. Jia, Z. Xu, L. Zhang, Y. Li, T. Zhao and J. Xu, *Appl. Surf. Sci.*, 2022, **592**, 153170.
- 263 K. Du, L. He, S. Song, J. Feng, Y. Li, M. Zhang, H. Li, C. Li and H. Zhang, *Adv. Funct. Mater.*, 2021, **31**, 2103275.
- 264 H. Dong, S. Kareem, X. Gong, J. Ruan, P. Gao, X. Zhou, X. Liu, X. Zhao and Y. Xie, *ACS Appl. Mater. Interfaces*, 2021, **13**, 23960–23969.
- 265 S. Lou, S. Si, L. Huang, W. Gan, B. Lan, J. Zhang, M. Li, T. Xuan and J. Wang, *Chem. Eng. J.*, 2022, **430**, 132680.
- 266 H. Lin, X. Zhang, L. Cai, J. Lao, R. Qi, C. Luo, S. Chen, H. Peng, R. Huang and C. Duan, *J. Mater. Chem. C*, 2020, **8**, 5594–5599.
- 267 C. Geng, S. Xu, H. Zhong, A. L. Rogach and W. Bi, *Angew. Chem., Int. Ed.*, 2018, **57**, 9650–9654.
- 268 P. Cheng, K. Han and J. Chen, *ACS Mater. Lett.*, 2022, 60–78.
- 269 X. Chen, M. Jia, W. Xu, G. Pan, J. Zhu, Y. Tian, D. Wu, X. Li and Z. Shi, *Adv. Opt. Mater.*, 2023, **11**, 2202153.
- 270 H. Zhao, Y. Li, B. Zhang, T. Xu and C. Wang, *Nano Energy*, 2018, **50**, 665–674.
- 271 H. Zhao, K. Chordiya, P. Leukkunen, A. Popov, M. Upadhyay Kahaly, K. Kordas and S. Ojala, *Nano Res.*, 2021, **14**, 1116–1125.
- 272 H. Wang, H. Zhang, J. Wang, Y. Gao, F. Fan, K. Wu, X. Zong and C. Li, *Angew. Chem., Int. Ed.*, 2021, **60**, 7376–7381.
- 273 M. Aamir, Z. H. Shah, M. Sher, A. Iqbal, N. Revaprasadu, M. A. Malik and J. Akhtar, *Mater. Sci. Semicond. Process.*, 2017, **63**, 6–11.
- 274 M. Becker and M. Wark, *J. Phys. Chem. C*, 2018, **122**, 3548–3557.
- 275 A. D'Annibale, R. Panetta, O. Tarquini, M. Colapietro, S. Quaranta, A. Cassetta, L. Barba, G. Chita and A. Latini, *Dalton Trans.*, 2019, **48**, 5397–5407.
- 276 X. Li, X. Zhong, Y. Hu, B. Li, Y. Sheng, Y. Zhang, C. Weng, M. Feng, H. Han and J. Wang, *J. Phys. Chem. Lett.*, 2017, **8**, 1804–1809.
- 277 K. Ahmad and S. M. Mobin, *Energy Technol.*, 2020, **8**, 1901185.
- 278 D. Ju, X. Zheng, J. Liu, Y. Chen, J. Zhang, B. Cao, H. Xiao, O. F. Mohammed, O. M. Bakr and X. Tao, *Angew. Chem., Int. Ed.*, 2018, **57**, 14868–14872.



- 279 D. Ju, G. Lin, H. Xiao, Y. Zhang, S. Su and J. Liu, *Sol. RRL*, 2020, **4**, 2000559.
- 280 M. I. Saidaminov, O. F. Mohammed and O. M. Bakr, *ACS Energy Lett.*, 2017, **2**, 889–896.
- 281 H. Lin, C. Zhou, Y. Tian, T. Siegrist and B. Ma, *ACS Energy Lett.*, 2018, **3**, 54–62.
- 282 T. Zhu and X. Gong, *InfoMat*, 2021, **3**, 1039–1069.
- 283 Q. Ba, A. Jana, L. Wang and K. S. Kim, *Adv. Funct. Mater.*, 2019, **29**, 1904768.
- 284 L. Romani, A. Bala, V. Kumar, A. Speltini, A. Milella, F. Fracassi, A. Listorti, A. Profumo and L. Malavasi, *J. Mater. Chem. C*, 2020, **8**, 9189–9194.
- 285 W. Bi, Z. Wang, H. Li, Y. Song, X. Liu, Y. Wang, C. Ge, A. Wang, Y. Kang, Y. Yang, B. Li and Q. Dong, *J. Phys. Chem. Lett.*, 2022, **13**, 6792–6799.
- 286 Z. Hong, W. K. Chong, A. Y. R. Ng, M. Li, R. Ganguly, T. C. Sum and H. Sen Soo, *Angew. Chem., Int. Ed.*, 2019, **58**, 3456–3460.
- 287 S.-K. Yu, Z.-R. Zhang, Z.-H. Ren, H.-L. Zhai, Q.-Y. Zhu and J. Dai, *Inorg. Chem.*, 2021, **60**, 9132–9140.
- 288 Z. Zhuang, C. Peng, G. Zhang, H. Yang, J. Yin and H. Fei, *Angew. Chem., Int. Ed.*, 2017, **56**, 14411–14416.
- 289 X. Song, G. Wei, J. Sun, C. Peng, J. Yin, X. Zhang, Y. Jiang and H. Fei, *Nat. Catal.*, 2020, **3**, 1027–1033.
- 290 D. Ju, G. Lin, M. Zhou, Y. Hua, X. Li, H. Li and J. Liu, *J. Mater. Chem. A*, 2022, **10**, 17752–17759.
- 291 C. Xue, Z.-Y. Yao, J. Zhang, W.-L. Liu, J.-L. Liu and X.-M. Ren, *Chem. Commun.*, 2018, **54**, 4321–4324.
- 292 X. Yang, L.-F. Ma and D. Yan, *Chem. Sci.*, 2019, **10**, 4567–4572.
- 293 I. Spanopoulos, I. Hadar, W. Ke, P. Guo, S. Sidhik, M. Kepenekian, J. Even, A. D. Mohite, R. D. Schaller and M. G. Kanatzidis, *J. Am. Chem. Soc.*, 2020, **142**, 9028–9038.
- 294 T. Sheikh, S. Maqbool, P. Mandal and A. Nag, *Angew. Chem., Int. Ed.*, 2021, **60**, 18265–18271.
- 295 G.-N. Liu, R.-Y. Zhao, B. Xu, Y. Sun, X.-M. Jiang, X. Hu and C. Li, *ACS Appl. Mater. Interfaces*, 2020, **12**, 54694–54702.
- 296 H. Peng, X. Wang, Y. Tian, T. Dong, Y. Xiao, T. Huang, Y. Guo, J. Wang and B. Zou, *J. Phys. Chem. Lett.*, 2021, **12**, 6639–6647.
- 297 D. A. Dougherty, *Acc. Chem. Res.*, 2013, **46**, 885–893.
- 298 O. M. Cabarcos, C. J. Weinheimer and J. M. Lisy, *J. Chem. Phys.*, 1998, **108**, 5151–5154.
- 299 Q. A. Akkerman, D. Meggiolaro, Z. Dang, F. De Angelis and L. Manna, *ACS Energy Lett.*, 2017, **2**, 2183–2186.
- 300 H. Liu, Z. Wu, J. Shao, D. Yao, H. Gao, Y. Liu, W. Yu, H. Zhang and B. Yang, *ACS Nano*, 2017, **11**, 2239–2247.
- 301 M. Lu, X. Zhang, Y. Zhang, J. Guo, X. Shen, W. W. Yu and A. L. Rogach, *Adv. Mater.*, 2018, **30**, 1804691.
- 302 M. Hamdan and A. K. Chandiran, *Angew. Chem., Int. Ed.*, 2020, **59**, 16033–16038.
- 303 Z. Xiao, H. Lei, X. Zhang, Y. Zhou, H. Hosono and T. Kamiya, *Bull. Chem. Soc. Jpn.*, 2015, **88**, 1250–1255.
- 304 S. Pont, D. Bryant, C.-T. Lin, N. Aristidou, S. Wheeler, X. Ma, R. Godin, S. A. Haque and J. R. Durrant, *J. Mater. Chem. A*, 2017, **5**, 9553–9560.
- 305 A. Aziz, N. Aristidou, X. Bu, R. J. E. Westbrook, S. A. Haque and M. S. Islam, *Chem. Mater.*, 2020, **32**, 400–409.
- 306 Q. Li, Z. Chen, I. Tranca, S. Gaastra-Nedea, D. Smeulders and S. Tao, *Appl. Surf. Sci.*, 2021, **538**, 148058.
- 307 P. Lin, A. Loganathan, I. Raifuku, M. Li, Y. Chiu, S. Chang, A. Fakharuddin, C. Lin, T. Guo, L. Schmidt-Mende and P. Chen, *Adv. Energy Mater.*, 2021, **11**, 2100818.
- 308 R. Babu, S. Bhandary, D. Chopra and S. P. Singh, *Chem. – Eur. J.*, 2020, **26**, 10519–10527.
- 309 Q. Jiang, D. Rebollar, J. Gong, E. L. Piacentino, C. Zheng and T. Xu, *Angew. Chem., Int. Ed.*, 2015, **54**, 7617–7620.
- 310 C.-C. Wang, J.-R. Li, X.-L. Lv, Y.-Q. Zhang and G. Guo, *Energy Environ. Sci.*, 2014, **7**, 2831–2867.
- 311 F. Wu, R. Pathak, J. Liu, R. Jian, T. Zhang and Q. Qiao, *ACS Appl. Mater. Interfaces*, 2021, **13**, 44274–44283.
- 312 A. Pisanu, A. Speltini, P. Quadrelli, G. Drera, L. Sangaletti and L. Malavasi, *J. Mater. Chem. C*, 2019, **7**, 7020–7026.
- 313 L. Romani, A. Speltini, F. Ambrosio, E. Mosconi, A. Profumo, M. Marelli, S. Margadonna, A. Milella, F. Fracassi, A. Listorti, F. De Angelis and L. Malavasi, *Angew. Chem., Int. Ed.*, 2021, **60**, 3611–3618.
- 314 L. Romani, A. Speltini, C. N. Dibenedetto, A. Listorti, F. Ambrosio, E. Mosconi, A. Simbula, M. Saba, A. Profumo, P. Quadrelli, F. De Angelis and L. Malavasi, *Adv. Funct. Mater.*, 2021, **31**, 2104428.
- 315 J. Liang, C. Wang, Y. Wang, Z. Xu, Z. Lu, Y. Ma, H. Zhu, Y. Hu, C. Xiao, X. Yi, G. Zhu, H. Lv, L. Ma, T. Chen, Z. Tie, Z. Jin and J. Liu, *J. Am. Chem. Soc.*, 2016, **138**, 15829–15832.
- 316 R. Chen, G. Gao and J. Luo, *Nano Res.*, 2022, 1–6.
- 317 D. Laishram, S. Zeng, K. M. Alam, A. P. Kalra, K. Cui, P. Kumar, R. K. Sharma and K. Shankar, *Appl. Surf. Sci.*, 2022, **592**, 153276.
- 318 M. V. Kovalenko, M. Scheele and D. V. Talapin, *Science*, 2009, **324**, 1417–1420.
- 319 J. Li, L. Xu, T. Wang, J. Song, J. Chen, J. Xue, Y. Dong, B. Cai, Q. Shan, B. Han and H. Zeng, *Adv. Mater.*, 2017, **29**, 1603885.
- 320 E. A. Muljarov, S. G. Tikhodeev, N. A. Gippius and T. Ishihara, *Phys. Rev. B: Condens. Matter Mater. Phys.*, 1995, **51**, 14370–14378.
- 321 H. Tsai, W. Nie, J.-C. Blancon, C. C. Stoumpos, R. Asadpour, B. Harutyunyan, A. J. Neukirch, R. Verduzco, J. J. Crochet, S. Tretiak, L. Pedesseau, J. Even, M. A. Alam, G. Gupta, J. Lou, P. M. Ajayan, M. J. Bedzyk, M. G. Kanatzidis and A. D. Mohite, *Nature*, 2016, **536**, 312–316.
- 322 I. C. Smith, E. T. Hoke, D. Solis-Ibarra, M. D. McGehee and H. I. Karunadasa, *Angew. Chem., Int. Ed.*, 2014, **53**, 11232–11235.
- 323 D. A. Hines and P. V. Kamat, *J. Phys. Chem. C*, 2013, **117**, 14418–14426.
- 324 W. Guan, Y. Li, Q. Zhong, H. Liu, J. Chen, H. Hu, K. Lv, J. Gong, Y. Xu, Z. Kang, M. Cao and Q. Zhang, *Nano Lett.*, 2021, **21**, 597–604.
- 325 Y. Wang, T. Wu, J. Barbaud, W. Kong, D. Cui, H. Chen, X. Yang and L. Han, *Science*, 2019, **365**, 687–691.



## Review

- 326 T. Takata, J. Jiang, Y. Sakata, M. Nakabayashi, N. Shibata, V. Nandal, K. Seki, T. Hisatomi and K. Domen, *Nature*, 2020, **581**, 411–414.
- 327 Y. Yang, M. Yang, D. T. Moore, Y. Yan, E. M. Miller, K. Zhu and M. C. Beard, *Nat. Energy*, 2017, **2**, 16207.
- 328 D. W. Wakerley, M. F. Kuehnel, K. L. Orchard, K. H. Ly, T. E. Rosser and E. Reisner, *Nat. Energy*, 2017, **2**, 17021.
- 329 S. Wang, B. Y. Guan and X. W. D. Lou, *J. Am. Chem. Soc.*, 2018, **140**, 5037–5040.
- 330 X.-D. Wang, Y.-H. Huang, J.-F. Liao, Y. Jiang, L. Zhou, X.-Y. Zhang, H.-Y. Chen and D.-B. Kuang, *J. Am. Chem. Soc.*, 2019, **141**, 13434–13441.
- 331 Y. Jiang, H. Chen, J. Li, J. Liao, H. Zhang, X. Wang and D. Kuang, *Adv. Funct. Mater.*, 2020, **30**, 2004293.
- 332 S. S. Bhosale, A. K. Kharade, E. Jokar, A. Fathi, S. Chang and E. W.-G. Diau, *J. Am. Chem. Soc.*, 2019, **141**, 20434–20442.
- 333 J. Sheng, Y. He, J. Li, C. Yuan, H. Huang, S. Wang, Y. Sun, Z. Wang and F. Dong, *ACS Nano*, 2020, **14**, 13103–13114.
- 334 J. Sheng, Y. He, M. Huang, C. Yuan, S. Wang and F. Dong, *ACS Catal.*, 2022, **12**, 2915–2926.
- 335 N. Li, X. Chen, J. Wang, X. Liang, L. Ma, X. Jing, D.-L. Chen and Z. Li, *ACS Nano*, 2022, **16**, 3332–3340.
- 336 R. Das, S. Chakraborty and S. C. Peter, *ACS Energy Lett.*, 2021, **6**, 3270–3274.
- 337 J. San Martin, N. Dang, E. Raulerson, M. C. Beard, J. Hartenberger and Y. Yan, *Angew. Chem., Int. Ed.*, 2022, **61**, e202205572.
- 338 D. Ricciarelli, W. Kaiser, E. Mosconi, J. Wiktor, M. W. Ashraf, L. Malavasi, F. Ambrosio and F. De Angelis, *ACS Energy Lett.*, 2022, **7**, 1308–1315.

